National Library of Canada
Acquisitions and Bibliographic Services Branch
395 Wellington Street
Ottawa, Ontario
K1A 0N4

Bibliothèque nationale du Canada
Direction des acquisitions et des services bibliographiques
395, rue Wellington
Ottawa (Ontario)
K1A 0N4

Your file Votre référence

Our file Notre référence

NOTICE

The quality of this microform is heavily dependent upon the quality of the original thesis submitted for microfilming. Every effort has been made to ensure the highest quality of reproduction possible.

If pages are missing, contact the university which granted the degree.

Some pages may have indistinct print especially if the original pages were typed with a poor typewriter ribbon or if the university sent us an inferior photocopy.

Reproduction in full or in part of this microform is governed by the Canadian Copyright Act, R.S.C. 1970, c. C-30, and subsequent amendments.

AVIS

La qualité de cette microforme dépend grandement de la qualité de la thèse soumise au microfilmage. Nous avons tout fait pour assurer une qualité supérieure de reproduction.

S'il manque des pages, veuillez communiquer avec l'université qui a conféré le grade.

La qualité d'impression de certaines pages peut laisser à désirer, surtout si les pages originales ont été dactylographiées à l'aide d'un ruban usé ou si l'université nous a fait parvenir une photocopie de qualité inférieure.

La reproduction, même partielle, de cette microforme est soumise à la Loi canadienne sur le droit d'auteur, SRC 1970, c. C-30, et ses amendements subséquents.

Canada

Covalent Modification of Cytochrome c with Tris(4,4'-dicarboxy-2,2'-bipyridine)ruthenium(II)

Hongtao Qi

A Thesis

in

The Department

of

Chemistry and Biochemistry

Presented in Partial Fulfilment of the Requirements
for the Degree of Master of Science at
Concordia University
Montreal, Quebec, Canada

May 1991

ISBN 0-315-81029-7

Canada

ABSTRACT

Covalent Modification of Cytochrome c

with Tris(4,4'-dicarboxy-2,2'-bipyridine)ruthenium(II)

Hongtao Qi

Tris(4,4'-dicarboxy-2,2'-bipyridine)ruthenium(II) [$Ru(dcbpy)_3^{4-}$] was covalently bound to horse heart cytochrome c (cyt c) via a carbodiimide and hydroxysulfosuccinimide coupling reaction at 0 °C. Gel filtration chromatography was used to separate cyt c and excess reagents. Unmodified cyt c and cyt c derivatives with Ru to heme ratios of 2:1 and 1:1 were separated by cation-exchange chromatography (CM-Sepharose). FPLC (cation-exchange) was used to further separate the 1:1 derivatives in which $Ru(dcbpy)_3^{4-}$ is attached to at least 10 different sites on cyt c. Quenching of the emission of $Ru(dcbpy)_3^{4-}$ by the heme in the derivatives indicates that $Ru(dcbpy)_3^{4-}$ is covalently bound to cyt c and that electron transfer may occur from the excited state of the ruthenium complex to the heme group. The maximum quenching rate constant (1.5×10^7 s^{-1}) is less than that reported for the $Ru(bpy)_2(dcbpy)$ derivatives of cyt c (3.8×10^7 s^{-1}). The sites of $Ru(dcbpy)_3^{4-}$ attachment on cyt c were investigated by FPLC using a reverse-phase column to separate the peptides from tryptic digests of two of the derivatives. The

FPLC chromatograms show that there are five Ru-containing fragments in the tryptic digests of the derivatives examined and three Ru peaks in the chromatogram of $Ru(dcbpy)_3^{4-}$ alone. It was further found that partial cleavage of bond between $Ru(dcbpy)_3^{4-}$ and cyt c occurs during the tryptic digestion. Amino acid analysis of the Ru-containing fragments identified the Ru attachment positions as lysine 86 and 87 in the two derivatives investigated.

ACKNOWLEDGEMENTS

Many thanks to Dr. A.M. English, my research thesis supervisor. I have greatly benefited from her comments and constructive criticisms. I would also like to thank the members of my Research Committee, Drs. P.H. Bird and O.S. Tee, whose advice and interest were helpful towards the completion of this thesis. Thanks to Ted Fox and Stephen Marmor for being helpful to me in my studies.

TABLE OF CONTENTS

LIST OF ABBREVIATIONS

AA	amino acid
BRI	Biotechnology Research Institute, National Research Council Canada
bpy	2,2'-bipyridine
CM-Sepharose	CM-Sepharose cation-exchange chromatography
cyt c	cytochrome c
dcbpy	4,4'-dicarboxy-2,2'-bipyridine
DEAE-Sepharose	DEAE-Sepharose anion-exchange chromatography
EDC	1-ethyl-3-(3-dimethylaminopropyl)carbodiimide hydrochloride
FPLC	fast protein liquid chromatography
G-25	G-25 gel filtration chromatography
HPLC	high performance liquid chromatography
NaAc	sodium acetate
$(NN)_3Ru(Lys)$cyt c	$Ru(dcbpy)_3^{4-}$ derivative of cyt c with Ru:heme = 1:1
$[(NN)_3Ru(Lys)]_2$cyt c	$Ru(dcbpy)_3^{4-}$ derivative of cyt c with Ru:heme = 2:1
P_i	phosphate buffer (from sodium salts)
$Ru(bpy)_2(dcbpy)$	bis(bipyridine)(4,4'-dicarboxybipyridine)ruthenium(II)
$Ru(dcbpy)_3^{4-}$	tris(4,4'-dicarboxy-2,2'-bipyridine)ruthenium(II)

sulfo-NHS	N-hydroxysulfosuccinimide
TFA	trifluoroacetic acid
TPCK	N-tosyl-L-phenylalanyl chloromethyl ketone

LIST OF FIGURES

LIST OF TABLES

1. Introduction

The relationship between electron transfer rate and distance between redox centres in metalloproteins is of much current interest [1,2]. The most direct way to address this problem is to measure the intramolecular electron transfer rate between redox centres of known separation [3-7]. Using small metal complexes covalently linked to a metalloprotein has proven to be invaluable in these studies. The strategy is to bind a redox active metal complex to a metalloprotein of known structure and determine the site of attachment. Then the rate-distance relationship can be examined.

Owing to their excellent redox behaviour, ruthenium complexes have been used to modify various metalloproteins. Intramolecular electron transfer studies have been carried out on ruthenium labelled cyt c [2-5, 8, 9], myoglobin [7, 9, 10], blue copper proteins [9, 11, 12, 13] and mixed-metal hybrid hemoglobins [14]. The intramolecular electron transfer was found to take place between a $Ru^{II}(NH_3)_5$ group attached to histidine 33 of cyt c and the ferric heme group with a rate constant of about 30-55 s^{-1} [3, 4]. This reaction has a driving force of 0.11 eV and a separation of about 12 Å. However, the rate of electron transfer from the ferrous heme group of cyt c to $Ru^{III}(NH_3)_4$(isonicotinamide)-histidine 33 was over 10^5 times slower than the above rate, although the driving force was larger (0.18 eV) [8]. It has been proposed that the specific protein structure between the donor and acceptor groups plays an important role in electron transfer [8].

Among various ruthenium complexes, ruthenium polypyridine complexes have been extensively studied [15-21]. A carboxylic acid group on the bipyridine can be covalently attached to the amino group of a lysine residue by forming an amide bond via a carbodiimide coupling reaction [22-23]. N-hydroxysulfosuccinimide (sulfo-NHS) enhances this coupling reaction at physiological pH [24].

Cyt c is an electron-transport protein and consists of a single polypeptide chain of 104 amino acid residues and a covalently attached heme group. The properties of cyt c are well known and the three-dimensional structure of the ferric horse heart cyt c has been elucidated by high resolution by X-ray crystallography [25]. The α-carbon skeleton of horse heart cyt c is shown in Fig.1 [26]. It is possible to prepare a large number of covalent derivatives because there are 19 lysine residues in horse heart cyt c. Once the site of attachment of the ruthenium complex is determined, the distance between two redox centres can be determined from the X-ray structure.

Recently, Pan et al. [27, 28] reported the preparation of singly-labelled bis(bipyridine)dicarboxybipyridineruthenium(II)-cyt c derivatives [$(bpy)_2$(dcbpy)Ru(Lys)cyt c]. In their two-step procedure, cyt c was first treated with the monoN-hydroxysuccinimide ester of free dcbpy, and the singly-labelled (dcbpy)(Lys)cyt c derivatives were then separated and purified. In the second step, the individual (dcbpy)(Lys)cyt c derivatives were treated with $Ru^{II}(bpy)_2CO_3$ to form singly-labelled [$(bpy)_2$(dcbpy)Ru(Lys)cyt c] derivatives. These derivatives

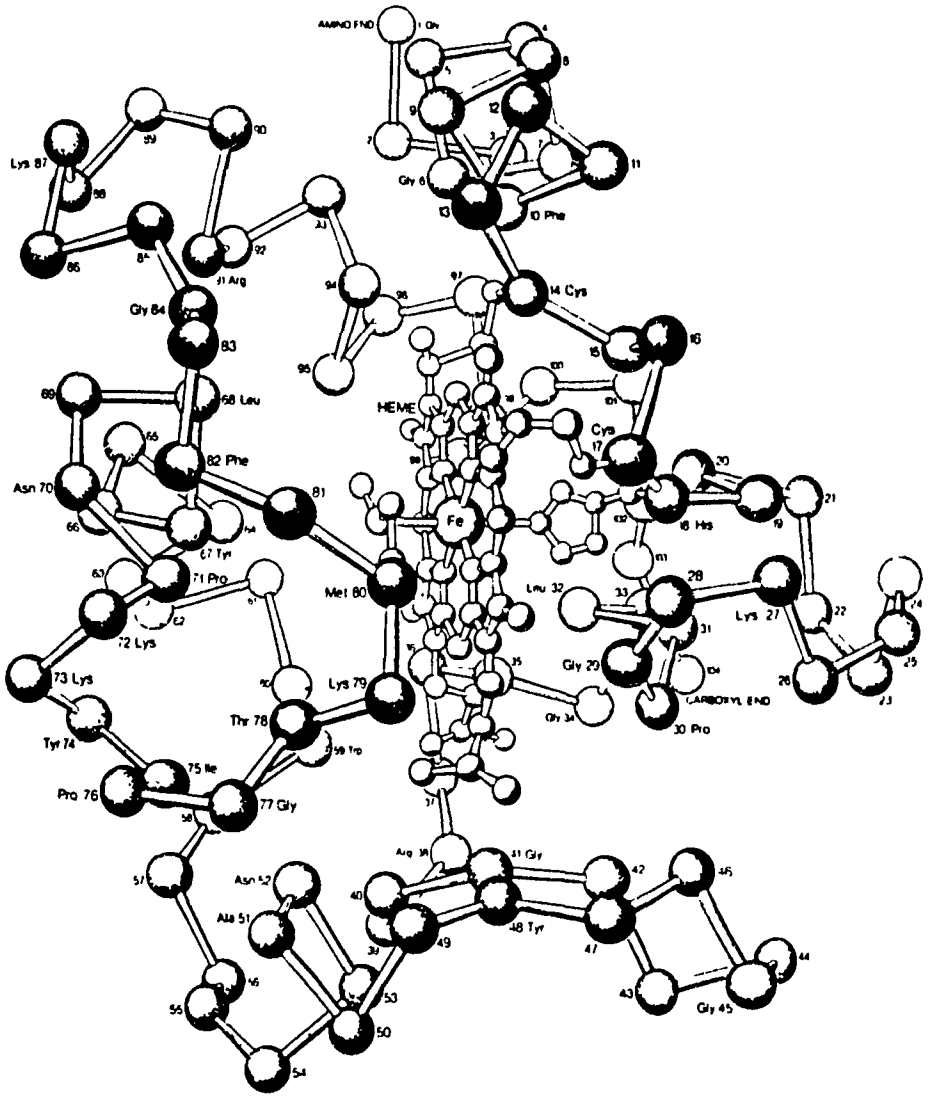

Fig.1. Alpha-carbon skeleton of horse heart cyt c (from Ref.26)

have a strong emission centred at 662 nm arising from the excited-state of the Ru complex, Ru^{II*}. Transient absorption spectroscopy was used to directly measure the rate constants for photoinduced electron-transfer from Ru^{II*} to the ferric heme group (k_1) and for the thermal back-reaction from the ferrous heme group to Ru^{III} (k_2). The rate constants were found to be: $k_1 = 0.3 - 20 \times 10^6\ s^{-1}$ and $k_2 = 0.6 - 30 \times 10^6\ s^{-1}$ for the derivatives modified at different lysines. The large electron-transfer rate constants observed for these derivatives are consistent with the large driving force ($\Delta E_1 = 0.98$ V, $\Delta E_2 = 1.05$ V) for electron transfer and the low reorganization energies of the $Ru(bpy)_2(dcbpy)$ complex and the cyt c heme [29].

This thesis reports the preparation and characterization of $Ru(dcbpy)_3^{4-}$ derivatives of cyt c. Section 2 gives the materials and methodology used, and the results and discussion are given in Sections 3 and 4, respectively.

2. Experimental Section

2.1. Materials

Horse heart cyt c (Type III and Type VI), 1-ethyl-3-(3-dimethylaminopropyl)carbodiimide hydrochloride (EDC) and trypsin (TPCK-treated) were obtained from Sigma. Ruthenium (III) chloride ($RuCl_3 \cdot H_2O$) was obtained from Alfa Products, and 4,4'-dicarboxy-2,2'-bipyridine (dcbpy) was purchased from Strem. 2,2'-bipyridine ruthenous dichloride hexahydrate [$Ru(bpy)_3 \cdot Cl_2 \cdot 6H_2O$] and 2,2'-bipyridine (bpy) were purchased from G. Frederick Smith Chemical Company, and N-hydroxysulfosuccinimide (sulfo-NHS) was from Pierce. Acetonitrile (CH_3CN; HPLC grade) and trifluoroacetic acid (TFA) were purchased from Fisher. All other chemicals were reagent grade and were used without further purification. G-25 gel filtration, CM-Sepharose cation-exchange, and DEAE-Sepharose anion-exchange resins were obtained from Pharmacia. YM-5 (5000 MW cutoff) ultrafiltration membranes were obtained from Amicon. Distilled water was purified by a NANO purification system (Sybron Barnstead).

The FPLC (Fast Protein Liquid Chromatography) system, including all parts [Pump:P500 (2), Controller: LCC-500PLUS, Monitor: UV-M, Valve: MV-7, MV-8, Column: Mono S HR5/5 (0.5x5 cm), PepRPC HR5/5 (0.5x5 cm), Fraction collector: FRAC-100], were from Pharmacia. The HP8451A UV-Vis diode array spectrophotometer and the Model RF-5000 spectrofluorophotometer were from Hewlett Packard and Shimadzu, respectively.

2.2. Methods

2.2.1. Synthesis and purification of $Ru(dcbpy)_3^{4-}$

$Ru(dcbpyH_2)_3Cl_2$ was synthesized from $RuCl_3$ and dcbpy by the following procedure: 0.35 mmol Ru (0.096 g $RuCl_3.3H_2O$), 1.35 mmol dcbpy (0.329 g) and 2 mmol $NH_2OH.HCl$ (0.14 g) were added to 25 ml H_2O in a round-bottom flask. The pH was adjusted with 0.5 M NaOH to pH 7, and the solution became a clear red colour. The reactant mixture was refluxed for 24 h at 90 °C. Then the solution was cooled to room temperature, the pH was adjusted to 5 with 2 N HCl and filtered to remove unreacted dcbpy. The filtered solution was then adjusted to pH 1 to protonate the dcbpy groups of the complex, and left standing at 4 °C overnight. Red $Ru(dcbpyH_2)_3.Cl_2$ crystals were obtained by centrifugation at 100xg and dried under vacuum. The crude product had absorbance ratios of $A_{206}/A_{304} = 1.04$ and $A_{304}/A_{466} = 3.65$.

Purification of the $Ru(dcbpy)_3^{4-}$ crystals was attempted using cation-exchange (CM-Sepharose), anion-exchange (DEAE-Sepharose) and gel filtration (G-25) chromatography. A 50 mg sample was added to 1 ml water and 1 drop of 1 N NaOH was added to dissolve the sample. The solution was loaded on the top of a 1.5x60 cm column (CM-Sepharose or G-25) and was eluted with 50 mM Pi buffer, pH 7 from the G-25 column, and 100 mM Pi, pH 7 from CM-Sepharose. A 1.5x18 cm column (DEAE-Sepharose) was used for anion-exchange chromatography and the sample was eluted with a solution containing 100 mM

NaAc and 400 mM NaCl, pH 3. The elution rate was 10 ml/h and the fraction size was 2 ml. The absorbance was measured at 206 and 466 nm.

$Ru(bpy)_2(dcbpy)$ was synthesized from $Ru(bpy)_2CO_3$ and dcbpy by the following procedure: 0.20 mmol $Ru(bpy)_2CO_3$ and 0.25 mmol dcbpy were added to 3 ml water and 5 ml ethanol. Two drops of a 1 g/ml $NH_2OH.HCl$ solution were added and the reaction mixture was refluxed for 8 h at 90 °C. The deep red solution was cooled and filtered, and ~0.5 ml of an aqueous solution of $NaClO_4$ (1 g/ml) was added to begin precipitation. The mixture was left standing overnight at 4 °C, and deep red crystals of $Ru(bpy)_2(dcbpy).(ClO_4)_2$ were obtained by centrifugation at 100xg and dried under vacuum.

2.2.2. Purification of commercial cyt c

Commercial cyt c contains some deamidated forms in which a number of glutamines and/or asparagines have been hydrolyzed to the corresponding acid [30]. These forms were removed prior to protein modification so that they do not complicate the purification of the Ru-modified cyt c.

A 50-150 mg sample of cyt c was dissolved in 2-5 ml water, and a pinch of solid $K_3Fe(CN)_6$ was added to the solution to insure complete oxidation of the protein. This solution was applied to a 1.5x60 cm CM-Sepharose cation-exchange column equilibrated with 100 mM Pi, pH 7. The flow rate was 30 ml/h, the fraction size was 10 ml, and the procedure was performed at 4 °C.

2.2.3. Coupling reaction of $Ru(dcbpy)_3^{4-}$ to cyt c

All reactants were mixed in 10 mM Pi, pH 8 to give the following final concentrations: 0.2 mM cyt c, 0.2-1.6 mM $Ru(dcbpy)_3^{4-}$, 6.8 mM sulfo-NHS, 10 mM EDC in a total volume of 2-20 ml. The mixture was stirred in an ice bath for 24 h. The reaction was terminated by removing the excess small reagents from cyt c. As a fluorescence control, a nonheme protein, lysozyme, was also modified with $Ru(dcbpy)_3^{4-}$. The procedure was the same as above but the reactant concentrations were adjusted to: 0.2 mM lysozyme, 0.2 mM $Ru(dcbpy)_3^{4-}$, 5 mM EDC and 3 mM sulfo-NHS and the reaction time was 2 h. The products from this reaction are indicated by $(NN)_3Ru(Lys)$lysozyme.

2.2.4. Purification and separation of the $Ru(dcbpy)_3^{4-}$ derivatives of cyt c

The excess small reagents were removed by ultrafiltration using a YM-5 filter and then by gel filtration on a 1.5x60 cm G-25 column equilibrated with 50 mM Pi, pH 7. The flow rate was 10 ml/h and the fraction size was 2 ml. The cyt c band from the G-25 column was concentrated to 1 ml by ultrafiltration (YM-5) and then applied to a 1.5x60 cm CM-Sepharose column equilibrated with 100 mM Pi, pH 7 to separate $(NN)_3Ru(Lys)$cyt c (Ru:heme = 1:1), $[(NN)_3Ru(Lys)]_2$ cyt c (Ru:heme = 2:1) and unmodified cyt c. The flow rate was 10 ml/h and the fraction size was 2 ml. All these procedures were performed at 4 °C. The band of $(NN)_3Ru(Lys)$cyt c from CM-Sepharose column was further separated by FPLC using a Mono S HR5/5 column equilibrated with 5 mM Pi, pH 6.0. Elution was carried out using linear Pi gradients, which were formed by mixing buffer A (5

mM Pi, pH 6.0) and buffer B (500 mM Pi, pH 6.0). The flow rate was 0.5 ml/min, the chart speed was 0.4 cm/ml, and absorbance was detected at 280 nm with an absorbance unit per full scale (AUFS) of 0.1.

2.2.5. Spectrophotometric determination of Ru/heme ratio

2.2.5.1. Ratio method

For a mixture of two components, if A_1 and A_2 are the absorbances at λ_1 and λ_2, and if A_1 and A_2 include contributions from both components, changing the relative amounts of the components will change A_1/A_2. $Ru(dcbpy)_3^{4-}$ has absorption maxima at 304 and 466 nm (Fig.5) and cyt c at 410 nm (Fig.7). Stock solutions of 10 mM $Ru(dcbpy)_3^{4-}$ and 10 mM native cyt c in 100 mM Pi, pH 7 were mixed to give a series of mixtures with 0-100 Ru%. Here, Ru% is the percent mole fraction of Ru [i.e., Ru% = 100Ru/(Ru+heme), where Ru and heme are the number of moles of the Ru complex and cyt c, respectively]. For example, a mixture of 3 ml of the $Ru(dcbpy)_3^{4-}$ solution and 7 ml of the cyt c solution gives Ru% = 30. Absorbances at 304, 466 and 410 nm were measured and the ratios, A_{304}/A_{410}, A_{410}/A_{466} were calculated. From these values, plots of Ru% vs. absorbance ratio were prepared. Since the resulting standard curves are independent of concentration, a comparison of the absorbance ratios measured for the $[(NN)_3Ru(Lys)]_n$cyt c derivatives with the standard values will yield the Ru% for the derivatives. Since heme% = 1-Ru%, the number of Ru per heme, the Ru/heme ratio, is given by the ratio Ru%/(1-Ru%).

2.2.5.2. Difference method

The absorbance of $[(NN)_3Ru(Lys)]_n$cyt c and native cyt c samples were matched at 410 nm, where cyt c has high absorbance and $Ru(dcbpy)_3^{4-}$ has low absorbance. A difference spectrum was obtained by subtracting the spectrum of cyt c from that of $[(NN)_3Ru(Lys)]_n$cyt c. The Ru content was calculated from the absorbance at 466 nm in the difference spectrum using an extinction coefficient (ε_{466}) of 14.1 mM^{-1} cm^{-1} for $Ru(dcbpy)_3^{4-}$ (see section 3.1). The heme content was calculated using ε_{410} = 106.1 mM^{-1} cm^{-1} for cyt c at 410 nm [31].

2.2.6. Steady-state emission measurements

The steady-state emission from 2 μM $Ru(dcbpy)_3^{4-}$, 2 μM $Ru(dcbpy)_3^{4-}$ in the presence of 2 μM cyt c, 2 μM $[(NN)_3Ru(Lys)]_n$cyt c, and 2 μM $[(NN)_3Ru(Lys)]$lysozyme were measured in 100 mM Pi, pH 7. All samples had the same absorbance at 466 nm (A_{466} = 0.048). Both excitation and emission slit widths were 10 nm and the pathlength was 1 cm. The excitation wavelength was 466 nm and the emission wavelength was 605 nm. The scan speed was super (60 nm/sec), sensitivity was high, and the response was auto. Since the reported emission maximum is 625 [32] and 618 nm [33], the emission spectra was also measured on a Perkin-Elmer MPF-44B Fluorometer. On excitation at 466 nm, the emission maximum was observed at 625 nm, in agreement with Ref.32.

2.2.7. Tryptic hydrolysis of native cyt c and $(NN)_3Ru(Lys)$cyt c

In order to identify the sites of $Ru(dcbpy)_3^{4-}$ attachment in $(NN)_3Ru(Lys)$cyt

c (i.e. the 1:1 Ru:heme derivatives), the proteins were digested by trypsin and the resulting peptides were separated by FPLC. Purified (Section 2.2.2) native cyt c (4 mg) was added to 2 ml of 0.2 M NH_4HCO_3 (pH 8) and digested at 37 °C for 20 h following addition of 40 µl trypsin solution (2 mg/ml in 0.001 M HCl) to give a trypsin-to-cyt c ratio of 1 to 50 (w/w) [34]. After filtration through a 0.2 µm acrodisc filter (Gelman Sciences), the digested solution was injected into a FPLC PepRPC column to separate the peptides or flash frozen in liquid nitrogen and stored at -30 °C. The digestion procedure for FPLC of purified $(NN)_3Ru(Lys)$cyt c was the same as that for native cyt c except that 1 mg of sample was used.

2.2.8. Analysis of the tryptic peptides by FPLC

The digested peptides were separated by FPLC on a C_2-C_{18} reversed-phase column (PepRPC HR5/5; 0.5x5 cm). The column was equilibrated with 0.1% TFA in water and 100 µl of the digested sample were injected. The peptides were eluted with a linear CH_3CN gradient (0-35%) in 0.1% TFA at a flow rate of 0.8 ml/min. The absorbance was detected at 280 nm, 0.5 ml fractions were collected, and the chart speed was 0.8 cm/ml. The Ru-containing fractions were packed into sample bottles and sent to the Biotechnology Research Institute (BRI) for amino acid analysis.

3. Results

3.1. Purification of $Ru(dcbpy)_3^{4-}$

The structure of $Ru(dcbpy)_3^{4-}$ is shown in Fig.2. The anion and cation-exchange chromatograms of crude $Ru(dcbpy)_3^{4-}$ are given in Fig.3a and Fig.3b, respectively, and the gel filtration chromatogram is shown in Fig.4. Gel filtration on G-25 resulted in the separation of excess dcbpy from $Ru(dcbpy)_3^{4-}$ since the first band in Fig.4 is $Ru(dcbpy)_3^{4-}$, and the second band is free dcbpy. Ion-exchange chromatography did not separate excess dcbpy from $Ru(dcbpy)_3^{4-}$ completely as can be seen from the shoulders on the main bands in Fig.3.

The absorption spectra of dcbpy, unpurified and G-25 purified $Ru(dcbpy)_3^{4-}$ are shown in Fig.5. There are three main peaks (206, 304 and 466 nm) in the $Ru(dcbpy)_3^{4-}$ spectrum and two peaks (206 and 298 nm) in the dcbpy spectrum. If the $Ru(dcbpy)_3^{4-}$ sample contains free dcbpy, the ratio of A_{206}/A_{304} will increase since the dcbpy contribution is much more at 206 nm than at 304 nm. The ratio of A_{304}/A_{466} will also increase since free dcbpy has no absorbance at 466 nm. The absorbance ratios found for crude, anion-exchange, cation-exchange and G-25 purified $Ru(dcbpy)_3^{4-}$ are listed in Table 1.

The ratio of A_{304}/A_{466} for $Ru(dcbpy)_3^{4-}$ is dependent on the pH of the solution. Fig.6 shows the spectra of $Ru(dcbpy)_3^{4-}$ from pH 9.7 to 2.0. $Ru(dcbpy)_3^{4-}$ will precipitate when the pH is less than 1 so that the spectrum is not available. The values of A_{304}/A_{466} at different pH are also given in Table 1. At pH 9.7,

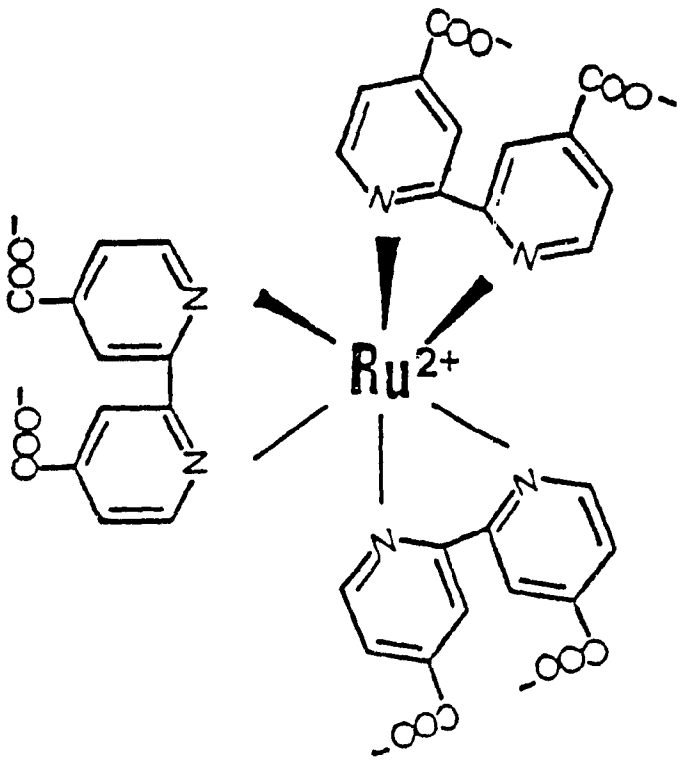

Fig.2. Structure of $Ru(dcbpy)_3^{4-}$

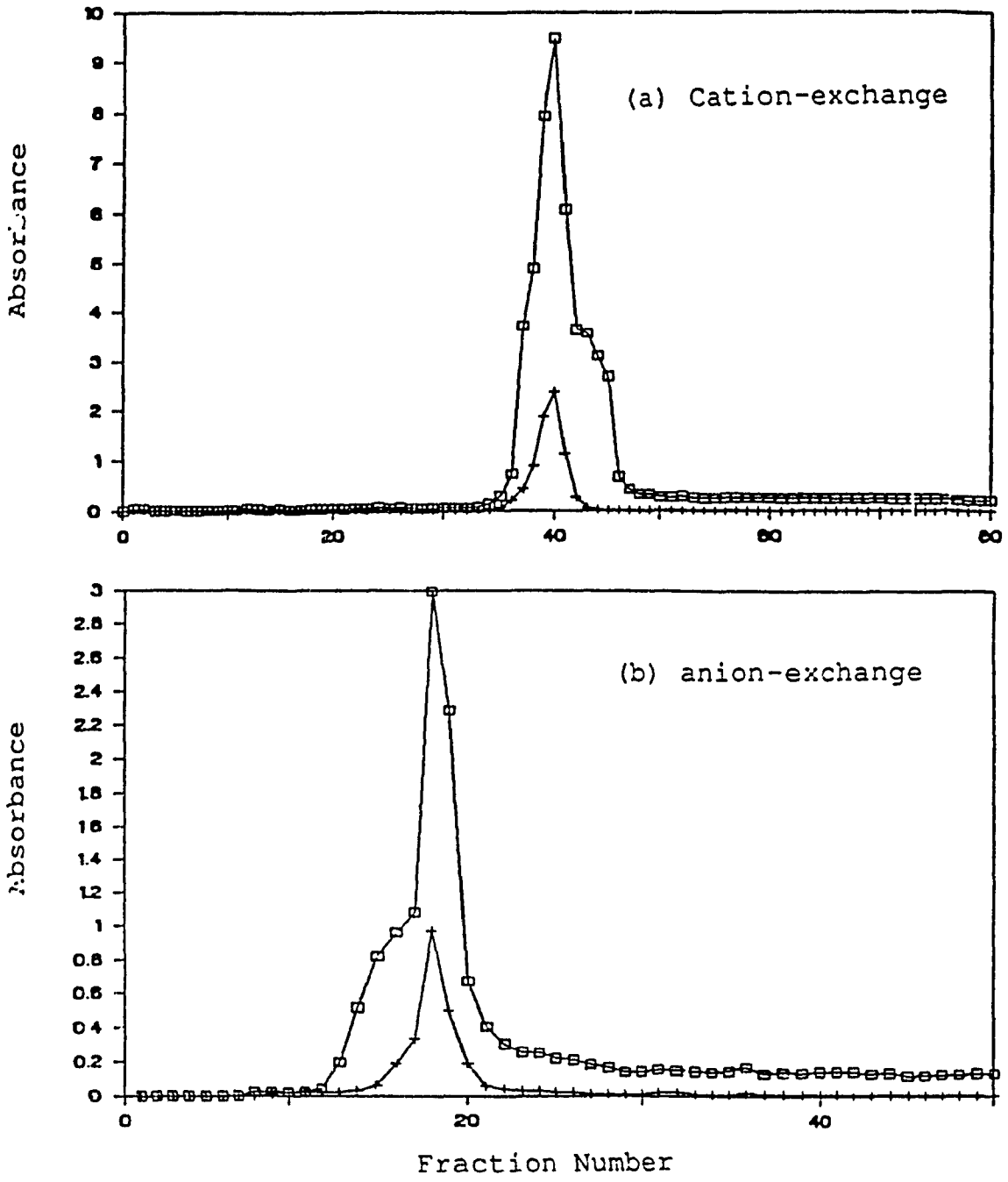

Fig.3. Purification of $Ru(dcbpy)_3^{4-}$ by cation-exchange (CM-Sepharose) and anion-exchange (DEAE-Sepharose) chromatography. Flow rate, 10 ml/h; fraction size, 2 ml. The absorbance of the fractions was read at 206 nm (□) and 466 nm (+). (a). 1.5x60 cm CM-Sepharose column; eluant, 100 mM Pi, pH 7. (b). 1.5x18 cm DEAE-Sepharose column; eluant, 100 mM NaAc with 400 mM NaCl, pH 3. The columns were equilibrated with the eluants prior to sample addition. The shoulders on the main bands are free dcbpy.

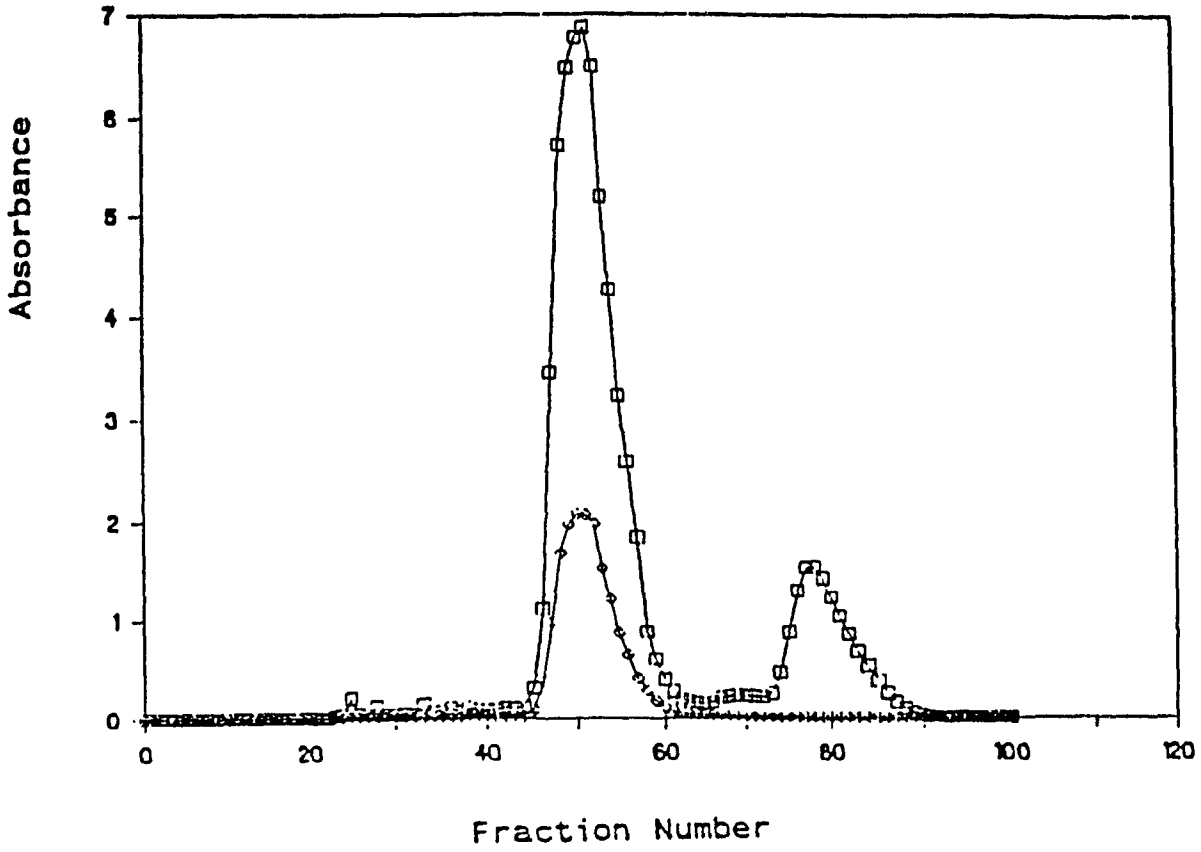

Fig.4. Purification of $Ru(dcbpy)_3^{4-}$ by gel filtration (G-25) chromatography. Column, 1.5x60 cm; eluant, 50 mM Pi, pH 7, flow rate, 10 ml/h; fraction size, 2 ml. The column was equilibrated with the eluant, and the absorbance of the fractions was read at 206 nm (□) and 466 nm (◇).

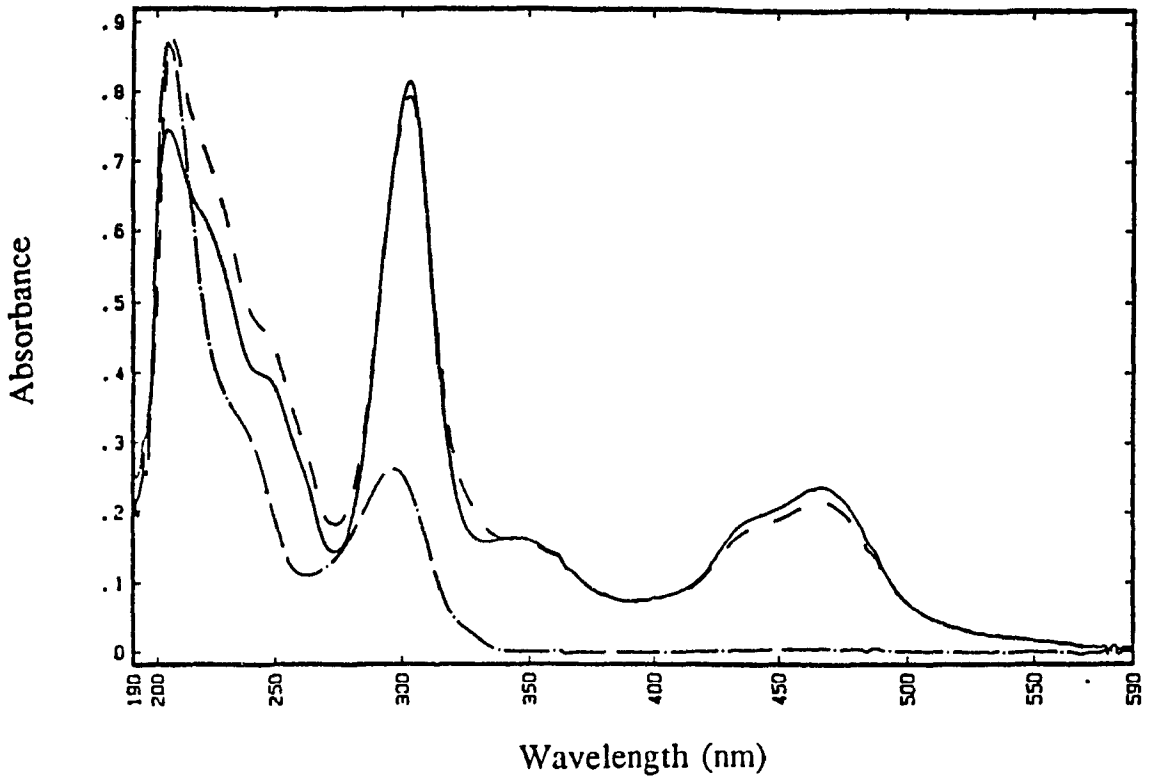

Fig.5. Absorption spectra of dcbpy (—— · ——), unpurified $Ru(dcbpy)_3^{4-}$ (— — —), and G-25 purified $Ru(dcbpy)_3^{4-}$ (————) in 100 mM Pi, pH 7

Table 1: Absorbance ratios for $Ru(dcbpy)_3^{4-}$ [a]

$Ru(dcbpy)_3^{4-}$ sample	A_{206}/A_{304}	A_{304}/A_{466}
crude	1.0-1.1	3.7-4.0
Purified by CM-Sepharose[b]	0.94	3.5
Purified by DEAE-Sepharose[c]	0.93	3.5
Purified by G-25[d]		
pH 9.7	0.86[e]	3.6
pH 7.0	0.91	3.4
pH 4.0		3.2[f]
pH 3.2		3.1[g]
pH 2.0		3.0[h]

[a] Absorbance was measured in 100 mM Pi, pH 7, except indicated.

[b] Fraction 41 in Fig.3(a)

[c] Fraction 18 in Fig.3(b)

[d] Fraction 51 in Fig.4

[e] A_{210}/A_{304}

[f] A_{304}/A_{468}

[g] A_{306}/A_{468}

[h] A_{308}/A_{470}

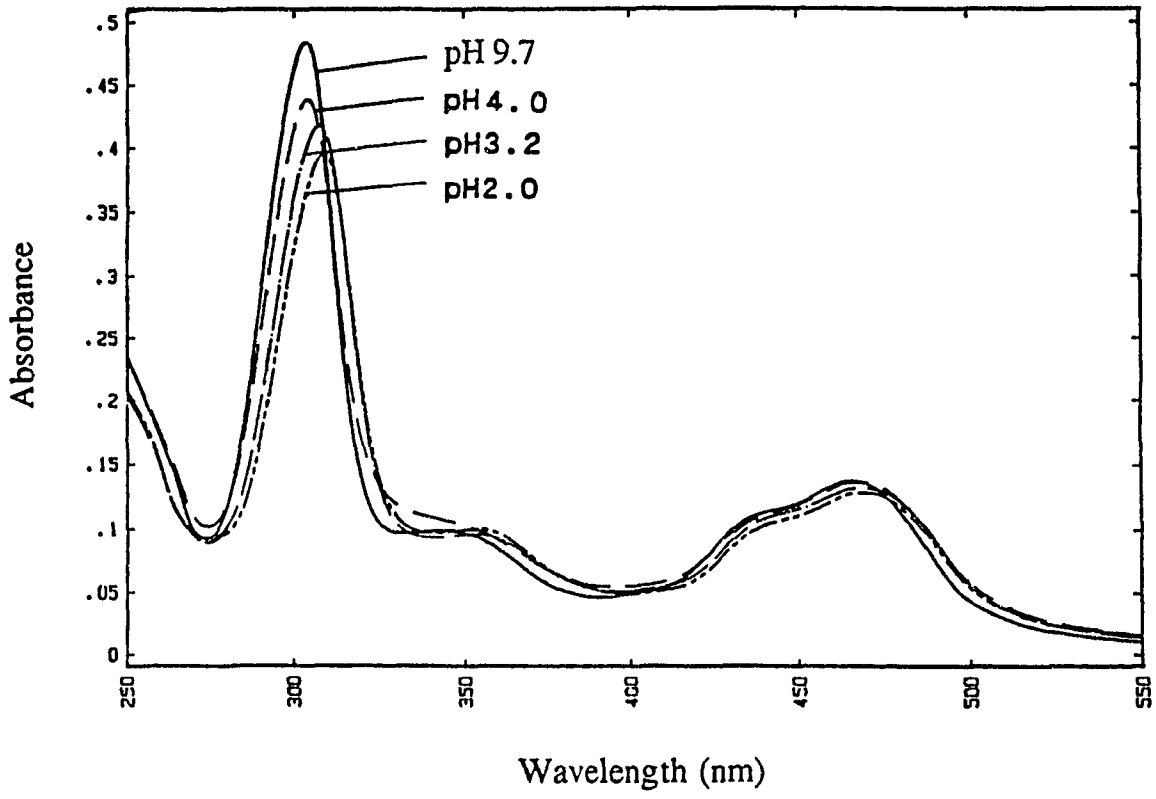

Fig.6. Absorbance spectra of $Ru(dcbpy)_3^{4-}$ at pH 9.7 (——————); pH 4.0 (—— —— ——); pH 3.2 (——— · ———); pH 2.0 (—— - - ——)

A_{304}/A_{466} = 3.58, which is very different from the reported value at the same pH (pH 9.7: A_{302}/A_{467} = 2.69) and similar to the value at pH 0.3 (A_{306}/A_{468} = 3.52) [33]; thus, it is possible that the reported values at pH 9.7 and 0.3 are interchanged.

From the data in Table 1, we assume that if $A_{206}/A_{304} > 0.91$ and $A_{304}/A_{466} > 3.4$ (pH 7), then the $Ru(dcbpy)_3^{4-}$ sample contains some free ligand. The extinction coefficients of the G-25 purified $Ru(dcbpy)_3^{4-}$ at 206, 304, and 466 nm were determined in 100 mM Pi (pH 7) from a Beer's Law plot and they are: ε_{206} = 44.4 mM^{-1} cm^{-1}, ε_{304} = 48.6 mM^{-1} cm^{-1}, ε_{466} = 14.1 mM^{-1} cm^{-1}.

3.2. Purification of commercial cyt c

The absorption spectrum of cyt c is shown in Fig.7. The CM-Sepharose chromatogram of commercial cyt c is given in Fig.8. The main peak is native cyt c and fractions before the main peak are deamidated forms. Fractions 41 to 54 were combined, and by cutting the peak and weighing, the yield of purified cyt c was estimated to be 70%.

3.3. Preparation of $[(NN)_3Ru(Lys)]_n$cyt c

The mechanism of the EDC coupling reaction is given in Fig.9. The water soluble carbodiimide, EDC catalyzes the formation of amide bonds between carboxylic acids and amines by activating the carboxylate to form an o-acylurea. When the reaction is carried out in aqueous medium, the o-acylurea intermediate

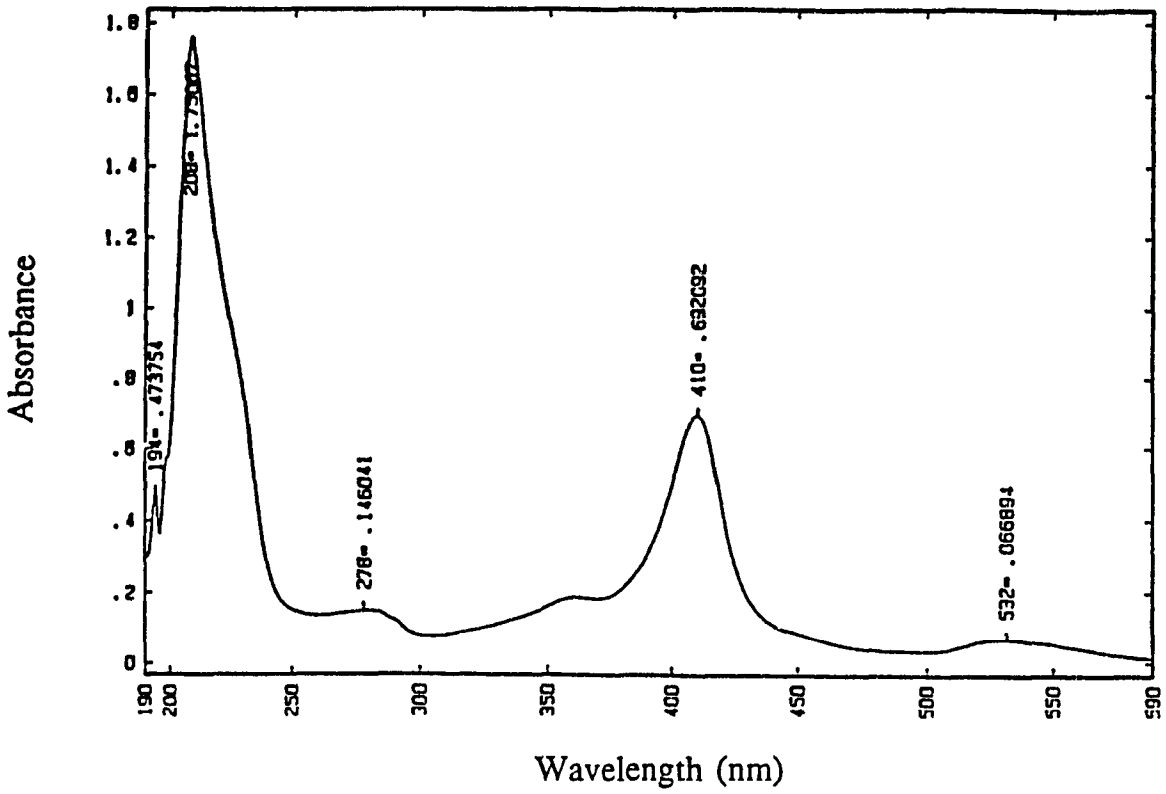

Fig.7. Absorption spectrum of horse heart ferricyt c in 100 mM Pi, pH 7

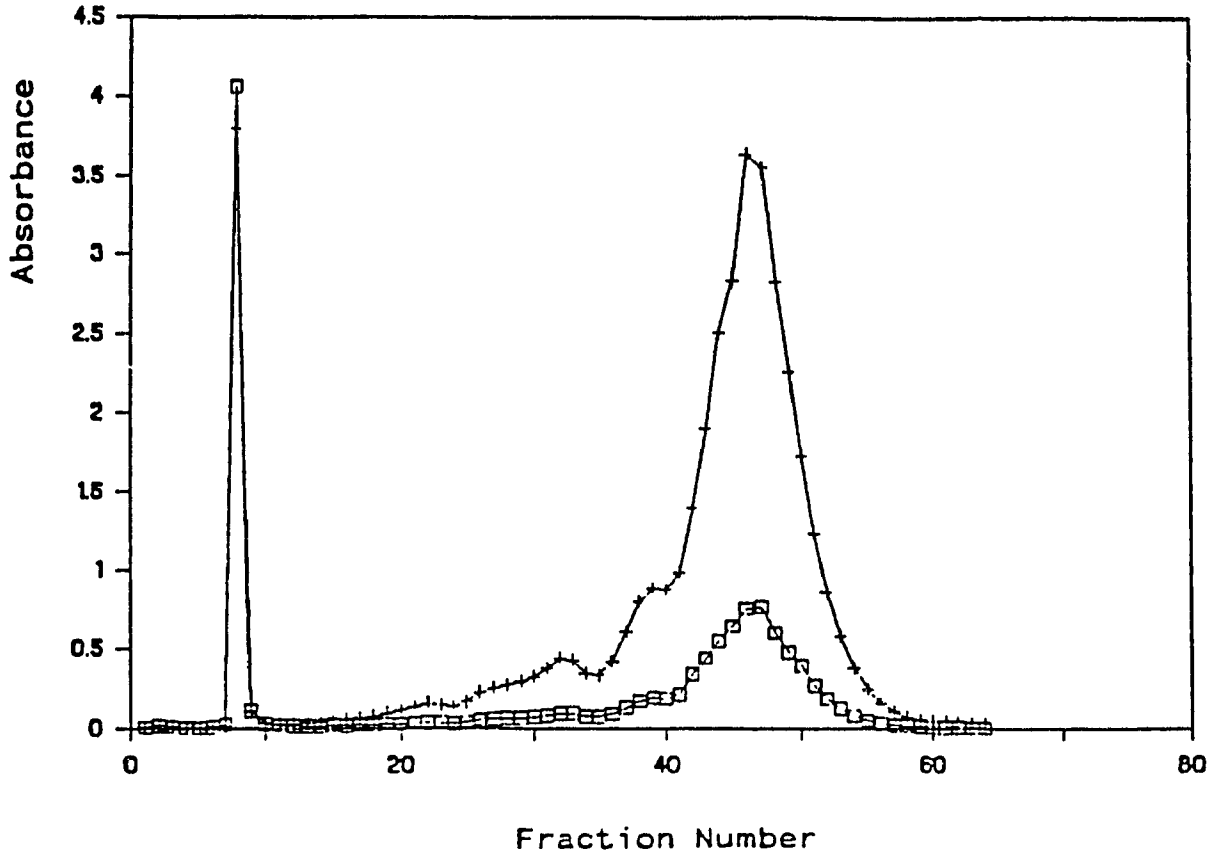

Fig.8. Purification of cyt c by cation-exchange (CM-Sepharose) chromatography. Column, 1.5x60 cm; eluant, 100 mM Pi, pH 7 at 4 °C; flow rate, 30 ml/h; fraction size, 10 ml. Column was equilibrated with the eluant, the absorbance was read at 280 nm (□) and 410 nm (+), and 50 mg of horse heart cyt c (type III) were applied to the column. The first sharp band is $K_3Fe(CN)_6$.

EDC only

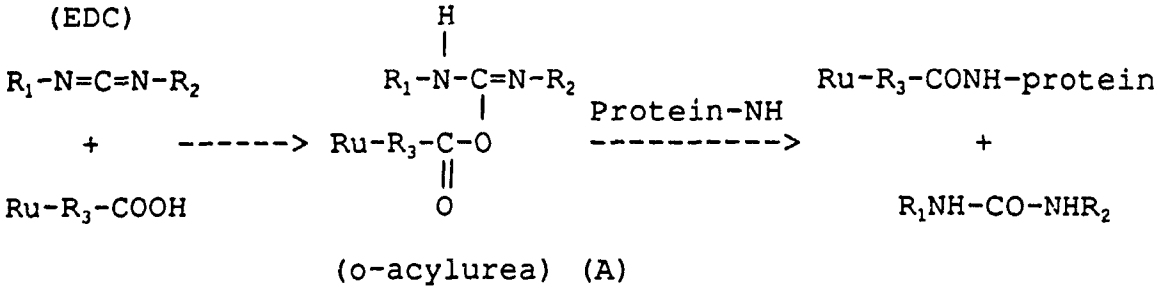

R_1 = CH_3CH_2-

R_2 = -$(CH_2)_3N(CH_3)_2$

R_3-COOH = dcbpy

sulfo-NHS enhanced carbodiimide reaction

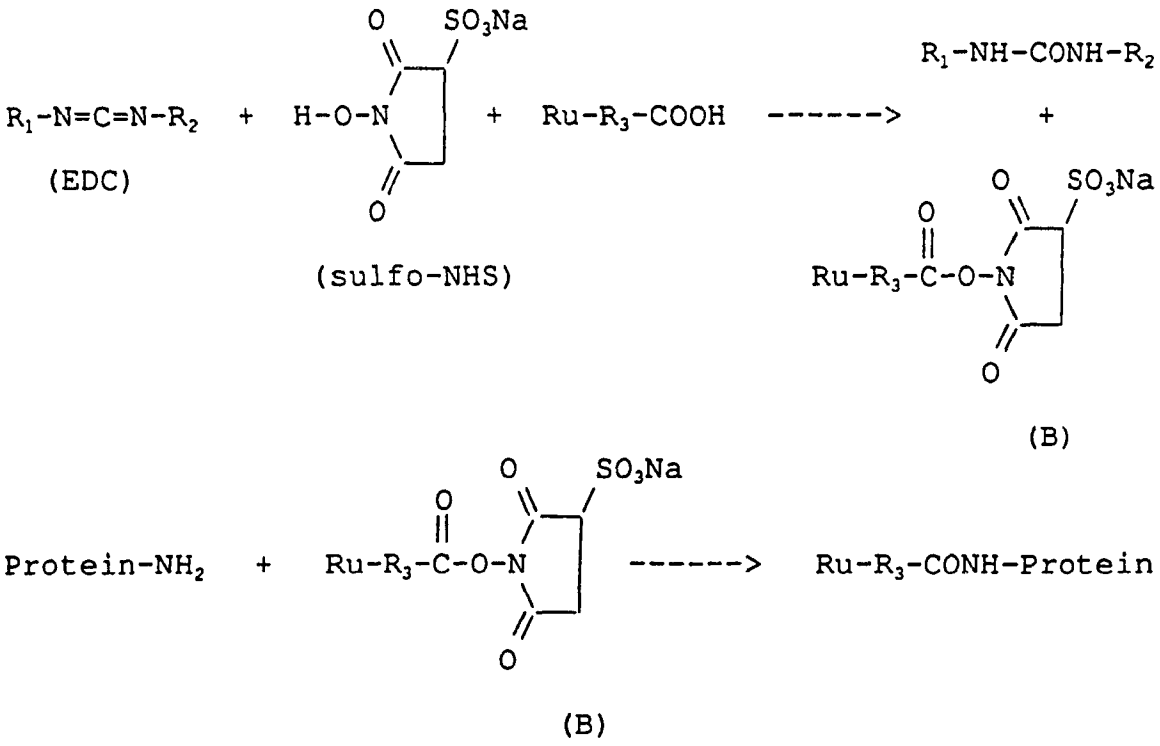

Fig.9 Mechanism of cyt c-Ru(dcbpy)$_3^{4-}$ coupling reaction

is subject to hydrolysis, resulting in decreased coupling efficiencies [22,23,24]. The addition of sulfo-NHS greatly enhances the yield of this reaction at physiological pH [24] by forming an active ester (B in Fig.9) which is more resistant to hydrolysis than the o-acylurea intermediate (A in Fig.9) and increases the coupling reaction yield.

The time course of the coupling reaction between cyt c and $Ru(dcbpy)_3^{4-}$ is given in Table 2 and Fig.10. Prolonging the reaction time increases the yield of modified cyt c but decreases the ratio of singly-modified (peak 2) to doubly-modified (peak 1) derivatives. The effect of changing the Ru to cyt c ratio in the coupling reaction is shown in Fig.11. Increasing the ratio of Ru to cyt c increases the yield of modified cyt c but again decreases the ratio of singly-modified (peak 2) to doubly-modified (peak 1) cyt c. The optimum reactant concentrations for the coupling reaction are: 0.5 mM $Ru(dcbpy)_3^{4-}$, 0.2 mM cyt c, 10 mM EDC and 6.8 mM sulfo-NHS, in 10 mM Pi, pH 8. Using these conditions the reaction was carried out at 0 °C for 24 h.

The EDC coupling of $Ru(dcbpy)_3^{4-}$ to lysozyme occurs at a higher rate than to cyt c. At the reactant concentrations given above, a precipitate formed in the lysozyme solution in only 30 min, indicating that lysozyme denatures under these conditions. Hence, the reactant concentrations were adjusted to 0.2 mM $Ru(dcbpy)_3^{4-}$, 0.2 mM lysozyme, 5 mM EDC and 3 mM sulfo-NHS in 10 mM Pi, pH 8, and the reaction was carried out at 0 °C for 2 h.

Table 2: Time course for the $Ru(dcbpy)_3^{4-}$-cyt c coupling reaction[a]

Time (h)	% Modified[b] cyt c	Ru/heme[c]	%Peak 1[d]	Ru/heme[c]	%Peak 2[d]
2	36	1.7	15	1.1	21
4	48	1.9	25	1.2	23
6	54	1.9	27	1.1	27
8	57	1.9	30	1.1	27
10	56	2.1	31	1.0	25
12	63	2.0	32	1.1	31
14	68	1.9	42	1.1	26
16	71	1.9	48	1.1	23
18	83	1.8	62	1.1	21
20	88	2.0	65	1.0	23
24	94	1.9	71	1.0	23
Average value		1.91±0.07		1.08±0.05	

[a] Experimental conditions: $Ru(dcbpy)_3^{4-}$ (1.6 mM), cyt c (0.2 mM), EDC (10 mM), and sulfo-NHS (6.8 mM) in 3 ml of 10 mM Pi, pH 8, 0 °C.

[b] Determined from the relative areas under the modified and native cyt c bands in the CM-Sepharose chromatogram (Fig.13).

[c] Determined as outlined in Section 3.5.

[d] Peak 1 and peak 2 were separated by CM-Sepharose chromatography and % peaks 1 and 2 were determined from the areas encompassed by the arrows in Fig.13.

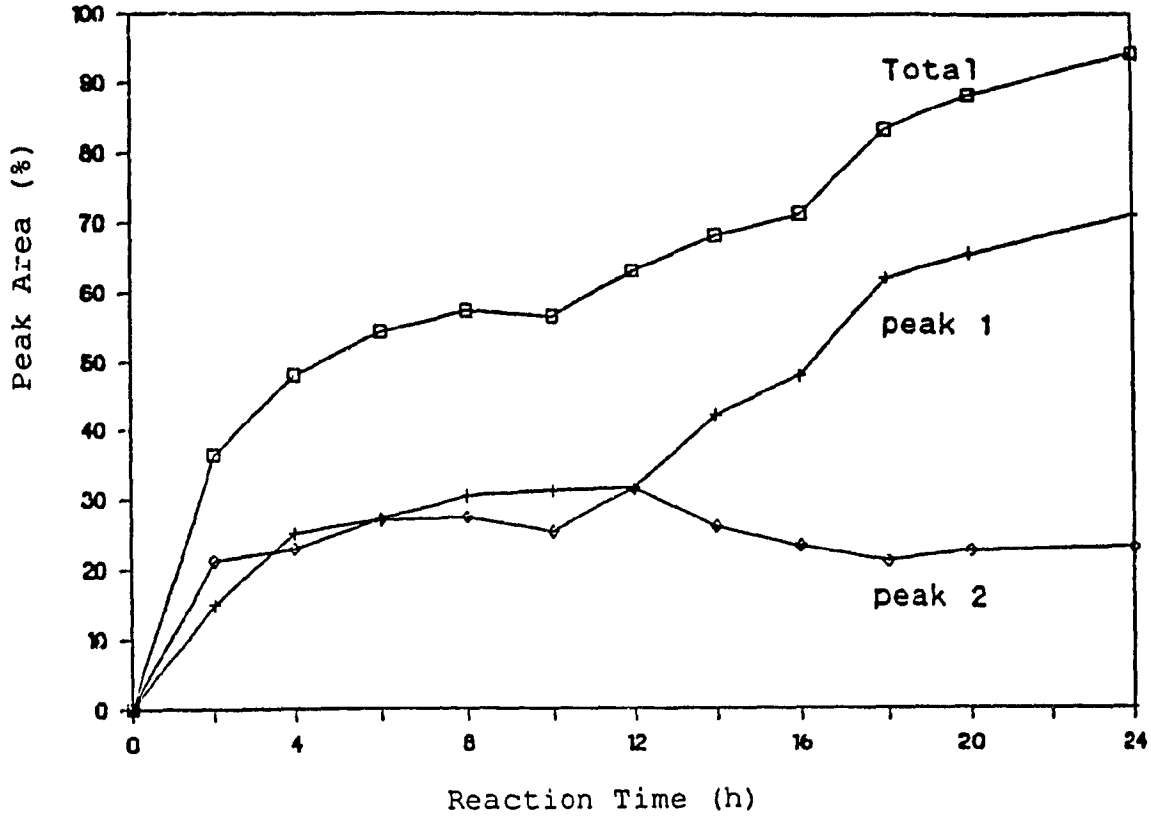

Fig.10. Percent cyt c modified vs. reaction time. Data are from Table 2; %modified cyt c (□); %peak 1 (+); %peak 2 (◇)

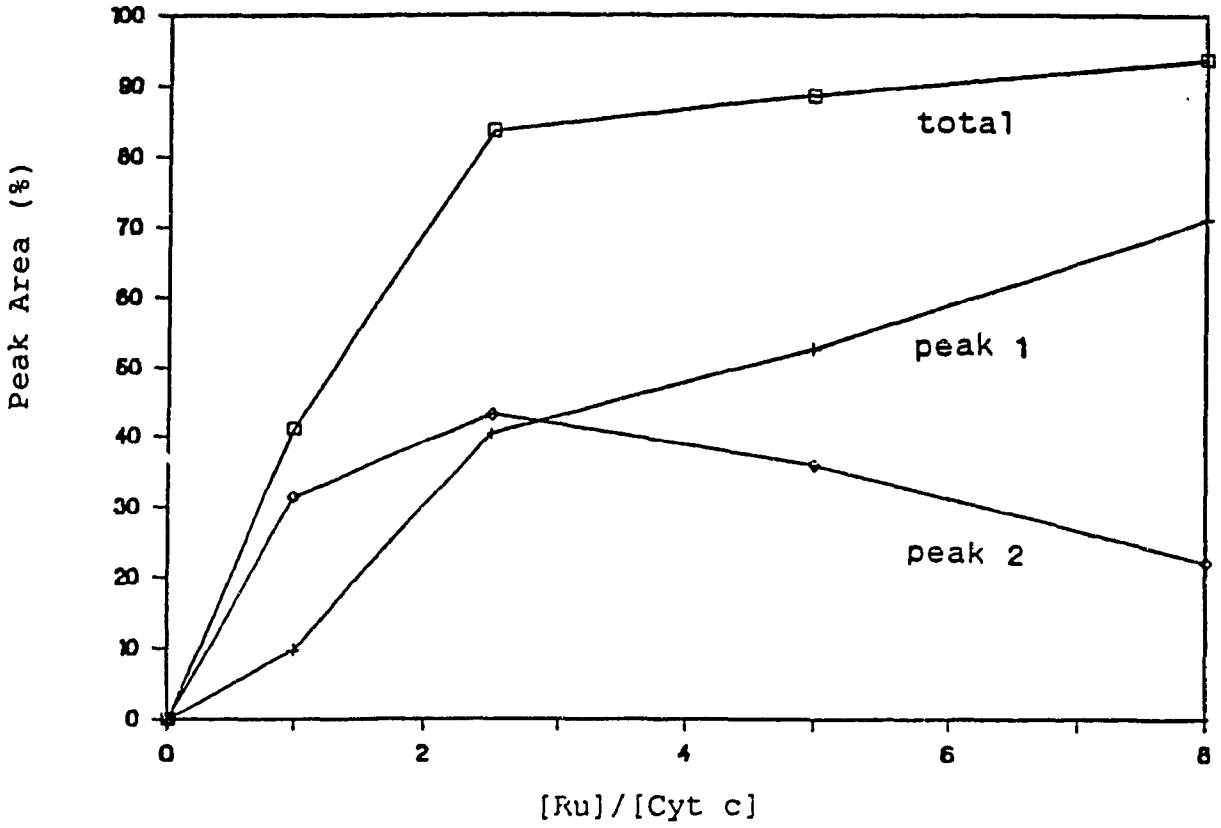

Fig.11. Percent cyt c modified vs. ratio of $Ru(dcbpy)_3^{4-}$ to cyt c in the coupling reaction. The EDC and sulfo-NHS concentration were kept at 10 and 6.8 mM, respectively, and the reaction was carried out at 0 °C for 24 h. Symbols as in the caption to Fig.10.

3.4. Cation-exchange separation of $[(NN)_3Ru(Lys)]_n$cyt c

The excess small reagents were removed by ultrafiltration (YM-5) and gel filtrations (G-25 and G-50), and the G-25 chromatogram is shown in Fig.12. The first band contains modified and unmodified cyt c, and the second band contains $Ru(dcbpy)_3^{4-}$ and the other small reactants. The G-50 and G-25 chromatograms were similar, indicating that no $Ru(dcbpy)_3^{4-}$-$(cyt\ c)_2$ derivatives were present. Cation-exchange chromatography (CM-Sepharose) was then used to separate the cyt c derivatives (Fig.13) according to their ruthenium to heme ratio. Derivatives with higher Ru/heme ratios have shorter retention times because $Ru(dcbpy)_3^{4-}$ binding decreases the positive charge of cyt c. There are two peaks in the CM-Sepharose chromatogram, peak 1 and peak 2, which are eluted before native cyt c (peak 3).

3.5. Analysis of ruthenium content peaks 1 and 2

The absorbance ratio method outlined in the experimental section was used to analyze the Ru content of peaks 1 and 2 of Fig.13. The absorption spectra of peaks 1 and 2, and native cyt c are shown in Fig.14, and the spectra of noncovalent mixtures of $Ru(dcbpy)_3^{4-}$ and cyt c are shown in Fig.15. Table 3 and Fig.16 give absorbance ratios vs. Ru% for noncovalent mixtures prepared as described in Section 2.2.5.1. Since these data are independent of concentration, we can obtain Ru% for $[(NN)_3Ru(Lys)]_n$cyt c by comparing their absorbance ratios with those of

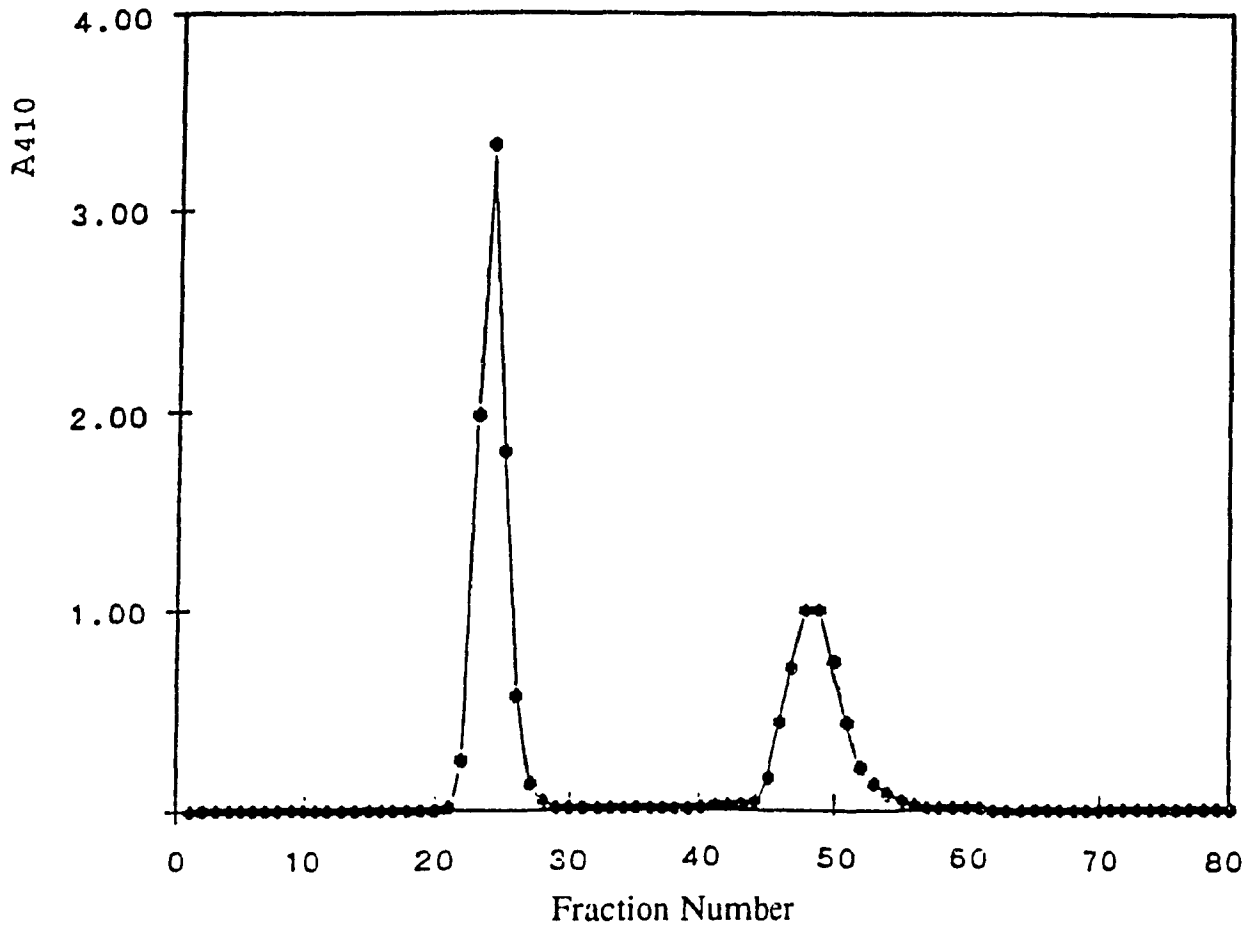

Fig.12. G-25 gel filtration of the $Ru(dcbpy)_3^{4-}$ and cyt c reaction mixture. Column, 1.5x60 cm; eluant, 50 mM Pi, pH 7, 4 °C; flow rate, 10 ml/h; fraction size, 2 ml. The column was equilibrated with the eluant, and the absorbance of the fractions was read at 410 nm. The first peak contains modified and unmodified cyt c, the second peak contains $Ru(dcbpy)_3^{4-}$ and other small reactants.

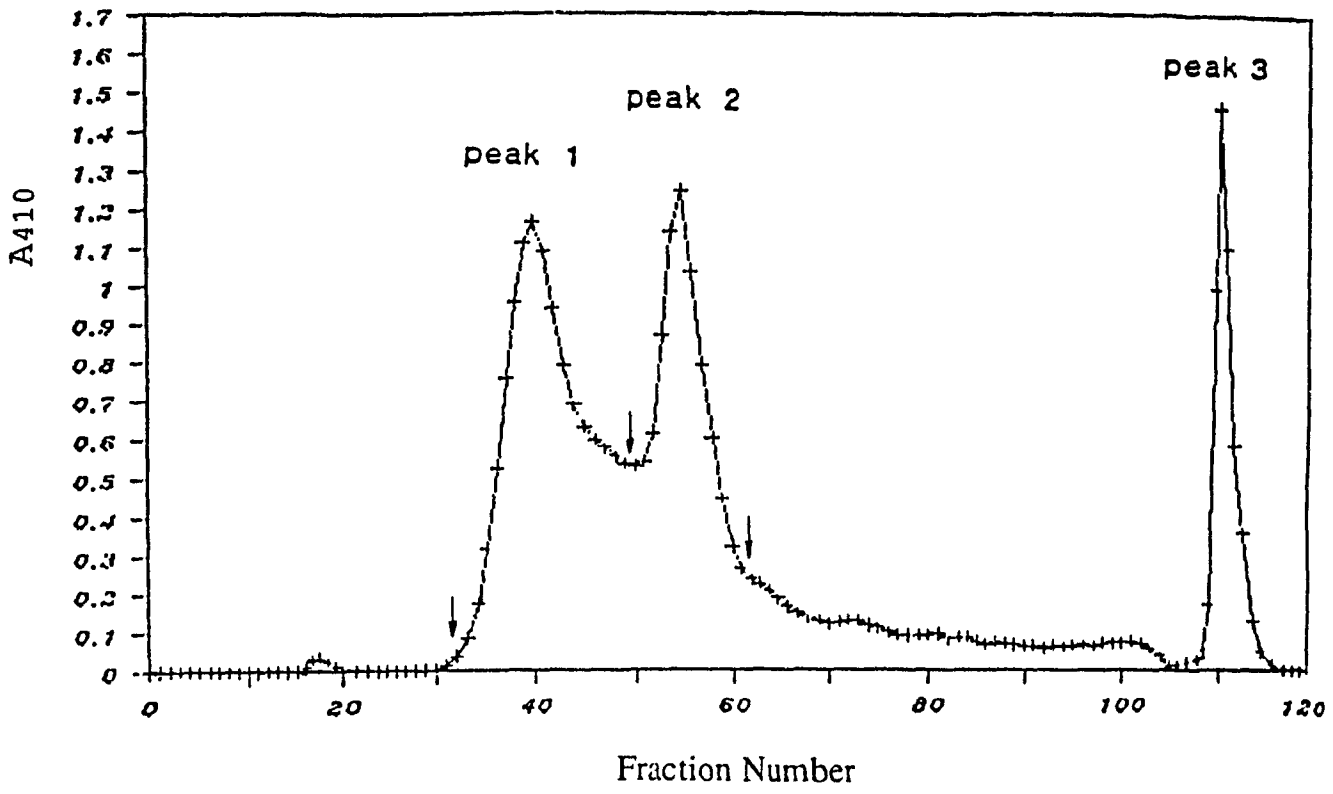

Fig.13. Separation of modified cyt c and unmodified cyt c on a 1.5x60 cm cation-exchange (CM-Sepharose) column equilibrated with 100 mM Pi, pH 7, 4 °C. Flow rate 10 ml/h, 2 ml fractions. Peaks 1 and 2 are cyt c derivatives with 2 Ru and 1 Ru per heme, respectively. Peak 3 is native cyt c. After fraction 70, 1 N NaCl was added the buffer to elute peak 3 from the column. The arrows indicate the peak areas used to obtain the % peak 1 and % peak 2 values given in Table 2.

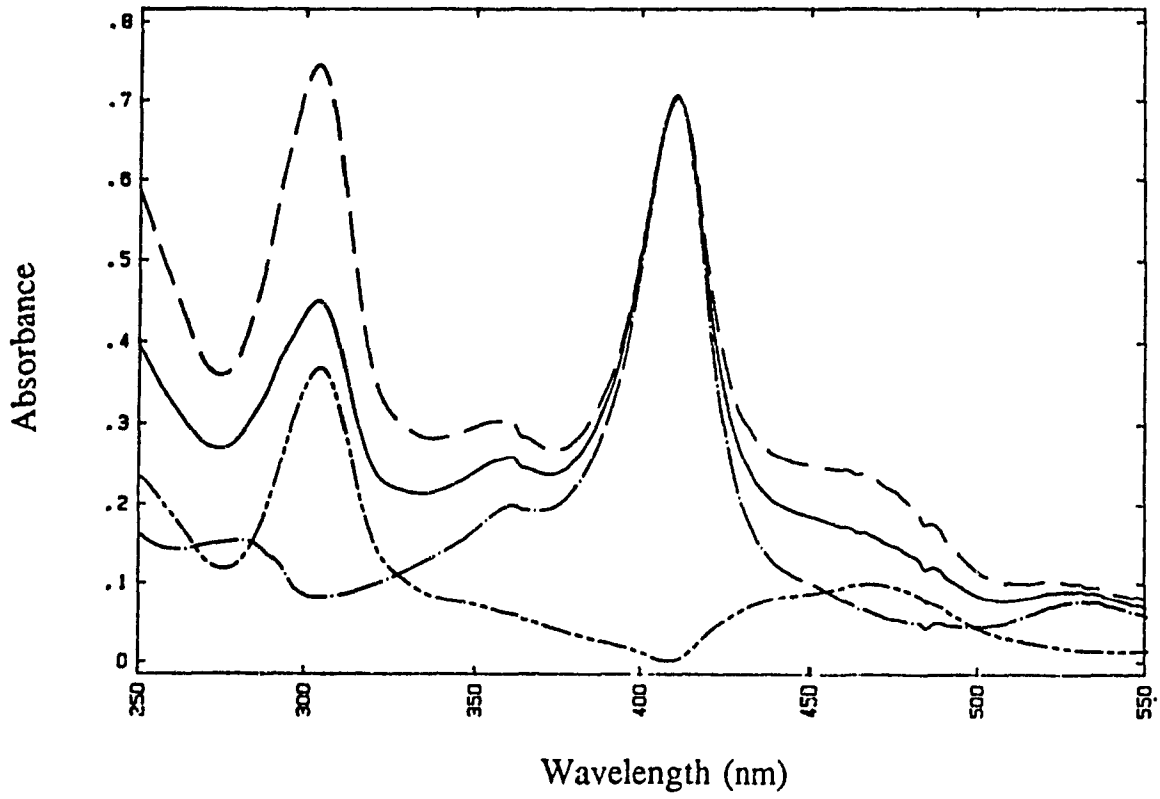

Fig.14. Absorption spectra in 100 mM Pi, pH 7 of peaks 1 (—— —— ——) and 2 (——————) from the CM-Sepharose column in Fig.13, and native cyt c (—— · ——) difference spectrum (peak 2-native cyt c) (—- - —- - —)

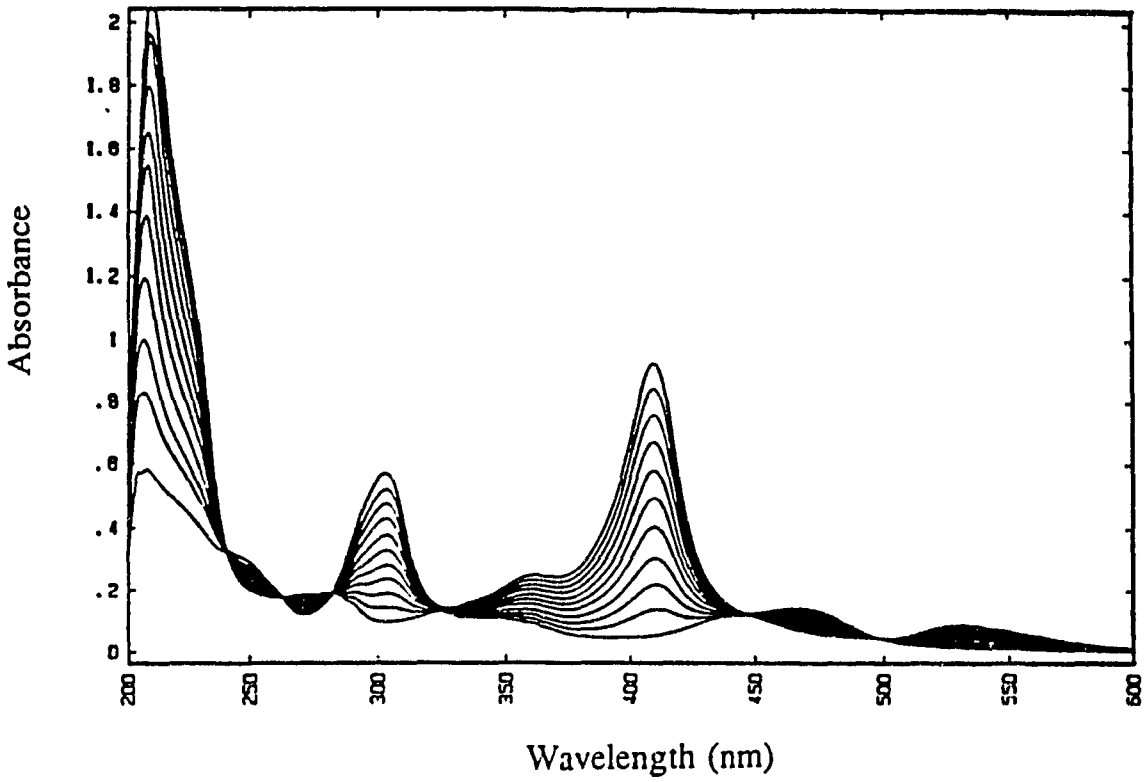

Fig 15. Absorbance spectra of noncovalent mixtures of $Ru(dcbpy)_3^{4-}$ and cyt c in 100 mM Pi, pH 7. The sum of $Ru(dcbpy)_3^{4-}$ and cyt c concentrations was fixed at 0.01 mM. The Ru% was varied from 0 to 100 [(Ru% = 100Ru/(Ru+heme)].

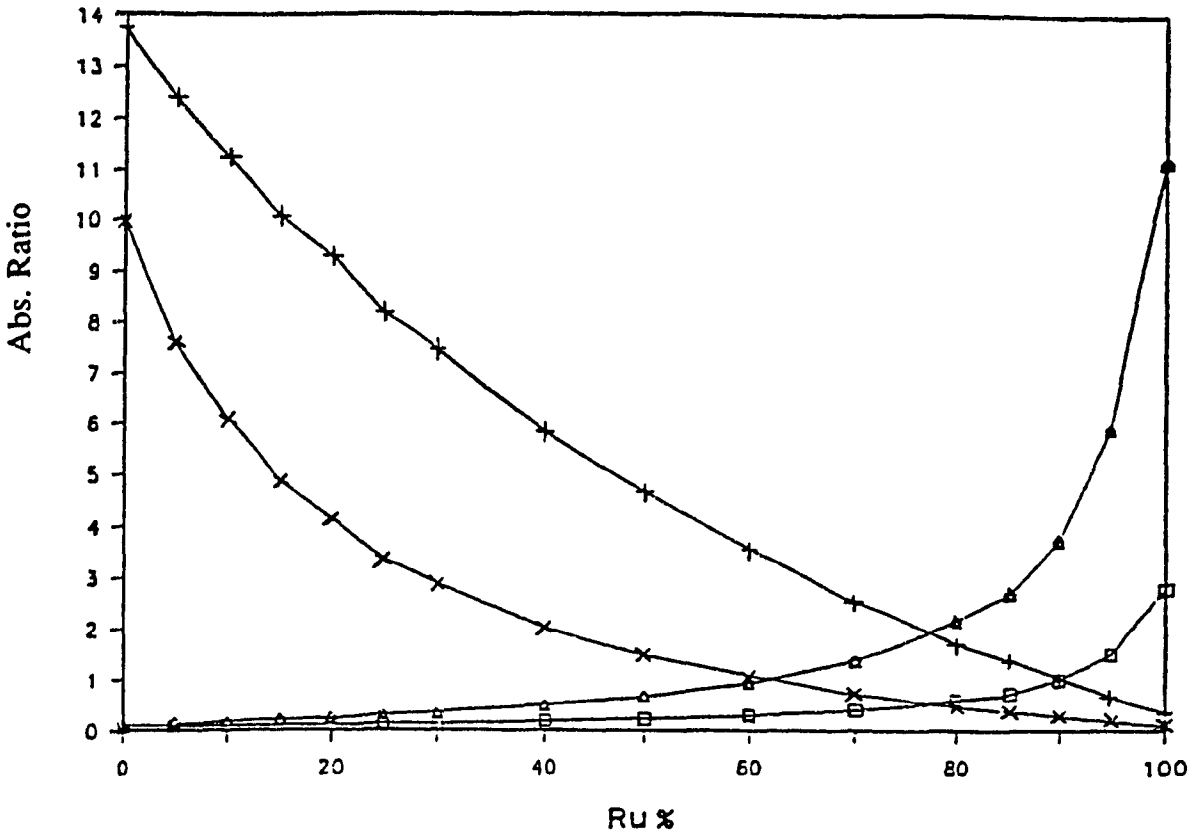

Fig.16. Plot of absorbance ratios vs. Ru%. The data are from Table 3, and the experimental conditions are given in the caption to Fig.15. □ A_{466}/A_{410}; + A_{410}/A_{466}; × A_{304}/A_{410}; Ω A_{410}/A_{304}

Table 3: Absorbance ratios for different Ru% values [a]

Ru%	A_{410}/A_{466}			A_{410}/A_{304}		
	Mean[b]	SD[b]	AD[b]	Mean[b]	SD[b]	AD[b]
0	13.74	0.284	0.267	9.977	0.328	0.295
5	12.40	0.029	0.026	7.602	0.047	0.040
10	11.24	0.130	0.122	6.087	0.079	0.007
15	10.05	0.052	0.049	4.876	0.037	0.035
20	9.296	0.034	0.030	4.150	0.083	0.079
25	8.182	0.029	0.028	3.385	0.008	0.007
30	7.480	0.122	0.108	2.911	0.080	0.073
40	5.830	0.130	0.122	2.032	0.036	0.034
50	4.661	0.049	0.046	1.498	0.052	0.046
60	3.575	0.054	0.051	1.075	0.007	0.006
70	2.551	0.029	0.019	0.718	0.001	0.001
80	1.719	0.010	0.009	0.464	0.002	0.002
85	1.396	0.014	0.013	0.371	0.002	0.002
90	1.012	0.010	0.008	0.263	0.003	0.003
95	0.664	0.010	0.009	0.170	0.004	0.003
100	0.357	0.012	0.010	0.090	0.003	0.002

[a] Ru% = 100Ru/(Ru+heme) is the percent mole fraction of Ru. The experimental conditions are given in the caption to Fig.15.

[b] Measurements were carried out in triplicate, SD = standard deviation, AD = average deviation.

the standards in Table 3 and Fig.16.

Fig.14 also shows the difference spectrum for $(NN)_3Ru(Lys)$cyt c. The Ru:heme ratios were also determined as described in Section 2.2.5.2. In order to compare the accuracies of the absorbance ratio and difference methods, solutions of known Ru% were prepared and analyzed by the two methods. The results, shown in Table 4, indicate that absorbance ratio method exhibits better accuracy and precision; thus, this method was used to determine the Ru content of the samples. As shown in Table 2 above, the average Ru/heme values for peaks 1 and 2 (Fig.13) are 1.91 ± 0.07 and 1.08 ± 0.05, respectively. Overlap of these peaks, as seen in Fig.13, reduces the Ru content of peak 1 and increase the Ru content of peak 2. A second CM-Sepharose column was run using 85 mM Pi, pH 7 as eluent and the analyses show that the Ru/heme ratio is 2.0 for peak 1 and 1.0 for peak 2.

3.6. FPLC of $(NN)_3Ru(Lys)$cyt c

Peak 2 from the CM-Sepharose column was further separated by FPLC using a Mono S HR5/5 cation-exchange column. The FPLC chromatogram of peak 2 is shown in Fig.17. Assuming that all the peaks contain derivatives with a 1:1 ratio of Ru to heme, the different retention times on the FPLC column indicate that $Ru(dcbpy)_3^{4-}$ is attached to different lysines on cyt c. Peaks 2-6, 2-7, 2-8, 2-9 and 2-10 of Fig.17 probably contain single derivatives because they could not be further separated using a more shallow gradient unlike peaks 2-1 to 2-5, which can be

Table 4: Comparison of spectrophotometric methods for determination of Ru content

Sample[a]	Theoretical Ru%	Experimental Ru%[b]	RE[c] (%)	SD[c]
Absorbance ratio method				
1	38.0	39.5	3.95	0.331
2	45.0	45.1	0.22	0.329
3	53.0	53.1	0.02	0.516
4	65.0	65.8	1.23	0.370
5	72.0	72.9	1.25	0.102
difference method				
1	38.0	34.8	-8.42	0.490
2	45.0	43.1	-4.22	0.665
3	53.0	50.0	-5.66	0.309
4	65.0	60.4	-7.14	1.682
5	72.0	68.6	-4.7	0.993

[a] The same samples were used in the two methods.

[b] Average of 5 readings for the absorbance ratio method, or 3 readings for the difference method.

[c] Relative error (RE) and standard deviation (SD) of the mean

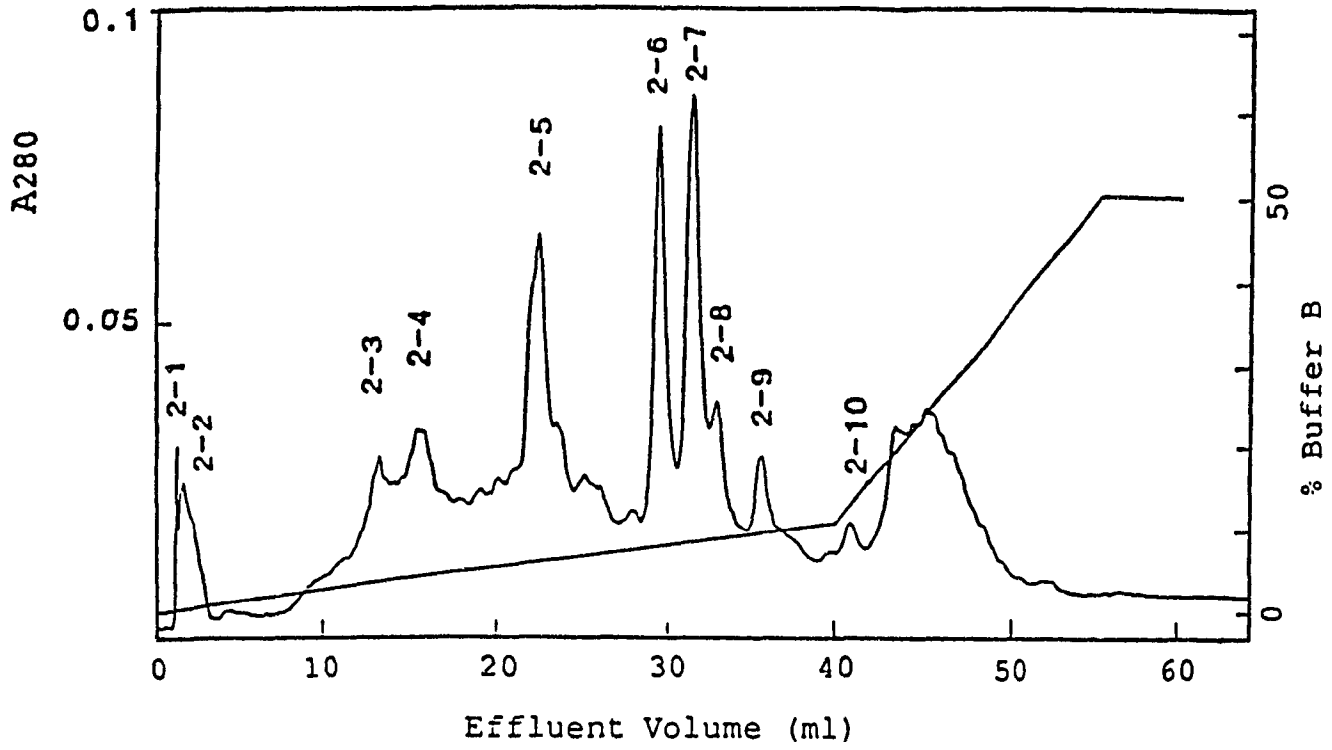

Fig.17. FPLC chromatogram of peak 2 from the CM-Sepharose column (Fig.13). Experimental conditions: FPLC Mono S HR5/5 column; eluant: buffer A , 5 mM Pi, pH 6, buffer B, 500 mM Pi, pH 6; linear gradients, 1% to 12% B from 0.5 to 40 ml effluent volume, and 12% to 50% B from 40 to 55 ml effluent volume; flow rate, 0.5 ml/min; chart speed, 0.4 cm/ml. Absorbance was monitored at 280 nm. The FPLC program is given in Appendix 1.

further separated. We focused on peaks 2-6 and 2-7 since they appear to be the major products. The capacity of HR5/5 column is ~0.2 mg protein so the automatic repetition program of the FPLC was used for scale up. Fig.18 shows the set up used, the resultant chromatograms are shown in Fig.19, and the FPLC program used is given in Appendix 2. Peaks 2-6 and 2-7 were further purified on the same column (Fig.20), and the yields of purified derivatives obtained from these peaks are given in Table 5.

The procedures used in the preparation and purification of $[(NN)_3Ru(Lys)]_n$cyt c are summarized in Fig.21.

$(NN)_3Ru(Lys)$lysozyme was also purified by gel filtration (G-25) and shows the same profile as $[(NN)_3Ru(Lys)]_n$cyt c. $(NN)_3Ru(Lys)$lysozyme was not further purified by ion-exchange chromatography since it was only used for emission control. The presence of unmodified lysozyme will not interfere with the emission intensity measurements of interest here. The yield of derivatized lysozyme and the $Ru(dcbpy)_3^{4-}$: lysozyme ratio were not determined.

3.7. Steady-state emission

The excitation spectra of peaks 2-6 and 2-7 (Fig.17) obtained by monitoring the emission at 605 nm are given in Fig.22, and the emission spectra obtained on excitation at 466 nm are given in Fig.23. The peaks in these spectra correspond to the $Ru^{II} \rightarrow$ dcbpy MLCT band at 466 nm, and the emission from the excited

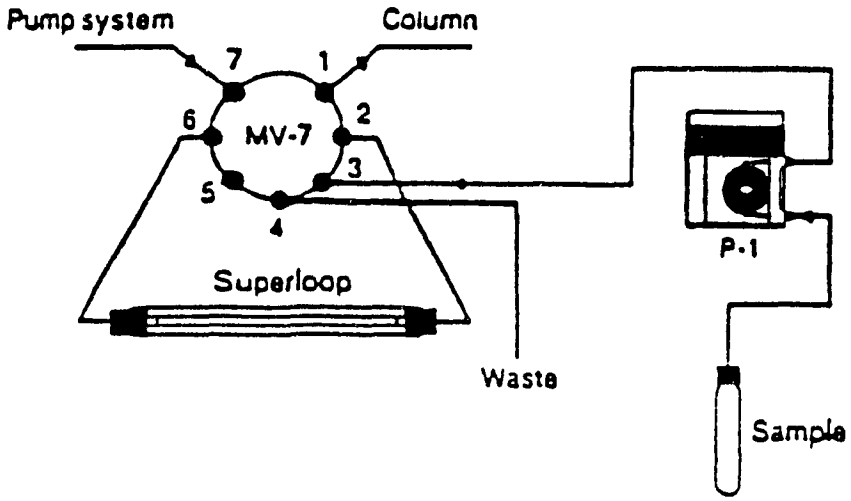

Fig.18. The components required for repeated sample injection. A peristaltic pump (P-1) loads the sample into the superloop (5 ml) via the motor valve MV-7. When MV-7 is in the "INJ" position (VALVE.POS 1.2: port 7-6-loop-2-1), 1 ml sample is injected into the column, then the valve is changed to the "LOAD" position (VALVE.POS 1.1: port 7-1). After the sample is eluted from the column, and the column is washed and equilibrated, the next 1 ml is automatically injected into the column and the cycle is repeated.

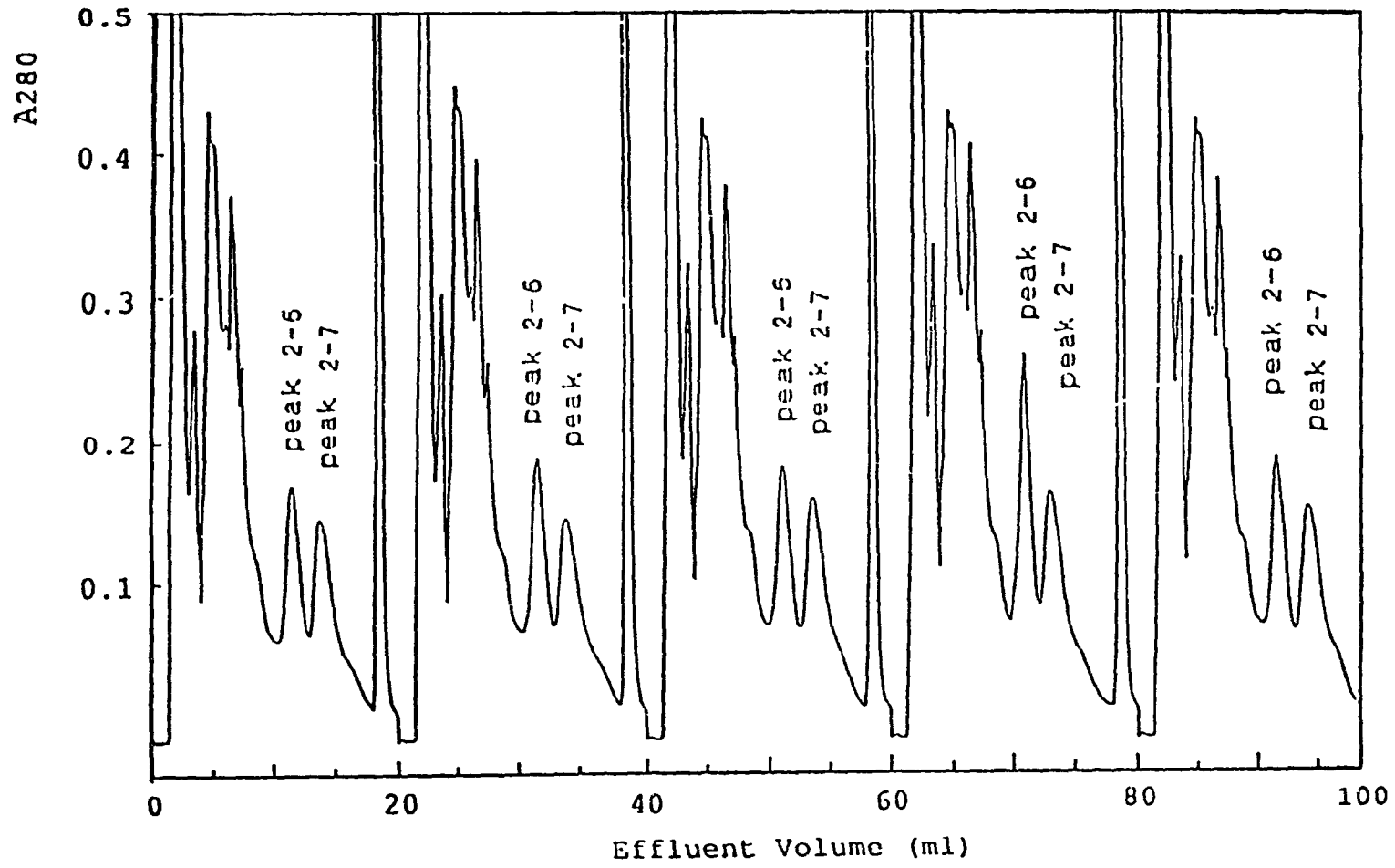

Fig.19. FPLC chromatograms of peak 2 using the automatic repetition program (see Fig.18 and Appendix 2). Buffer A, 5 mM Pi, pH 6; buffer B, 500 mM Pi, pH 6; flow rate, 0.5 ml/min; fraction size, 0.5 ml; chart speed, 0.4 cm/ml. Absorbance was monitored at 280 nm.

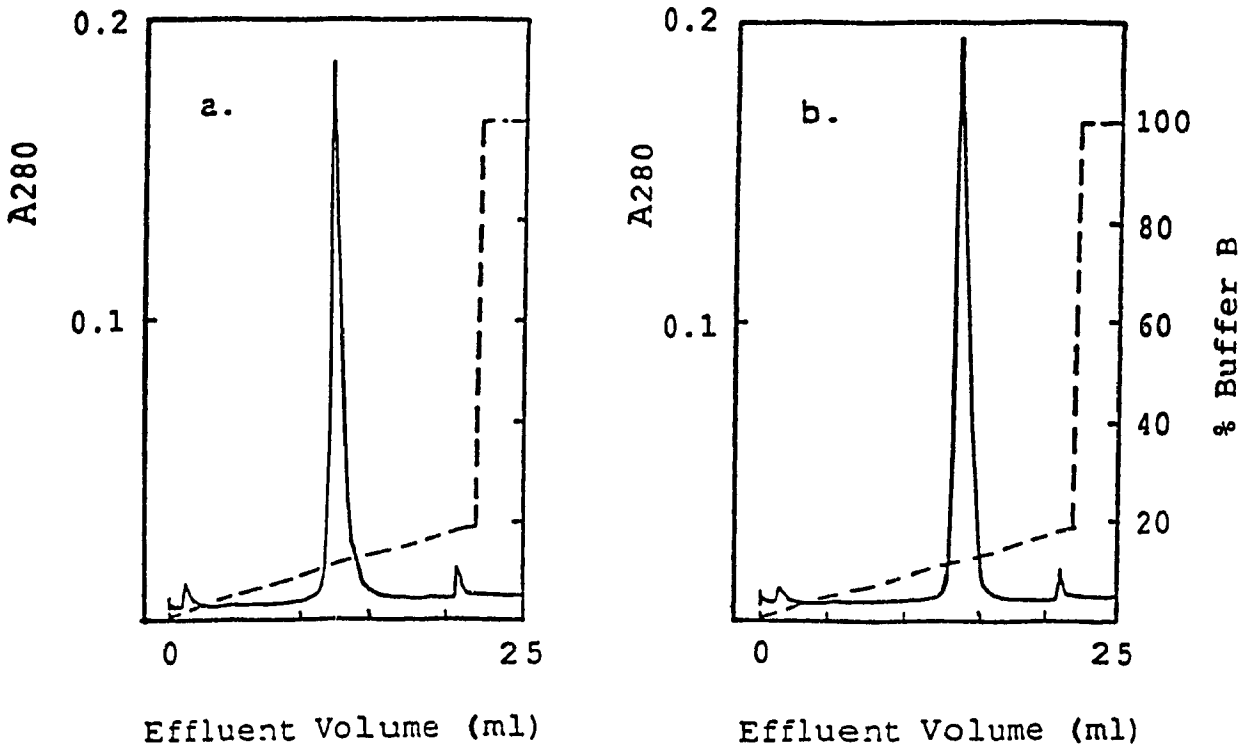

Fig.20. Rechromatography by FPLC of peaks 2-6 and 2-7 shown in Fig.19. Column, Mono S HR5/5; buffer A, 5 mM Pi, pH 6; buffer B, 500 mM Pi, pH 6; flow rate, 0.5 ml/min; chart speed, 0.4 cm/ml; Absorbance was monitored at 280 nm. The FPLC program is given in Appendix 3. (a). Peak 2-6 (b). Peak 2-7

Table 5: Yields of $Ru(dcbpy)_3^{4-}$ derivatives of cyt c

Process	Derivative	Yield(%)
cyt c purification[a]	native cyt c	70
coupling reaction [b] and CM-Sepharose	peak 1	41
	peak 2	43
FPLC	peak 2-6	9
	peak 2-7	9
overall yield [c]	peak 2-6	3
	peak 2-7	3

[a] Native cyt c from main peak of Fig.8.

[b] Reaction conditions were: 0.5 mM $Ru(dcbpy)_3^{4-}$, 0.2 mM cyt c, 10 mM EDC, 6.8 mM sulfo-NHS. The reaction was carried out in 10 mM Pi, pH 8, 0 °C for 24 h.

[c] Overall yield based on starting quantity of unpurified cyt c used (yield% = 70x43x9 = 3)

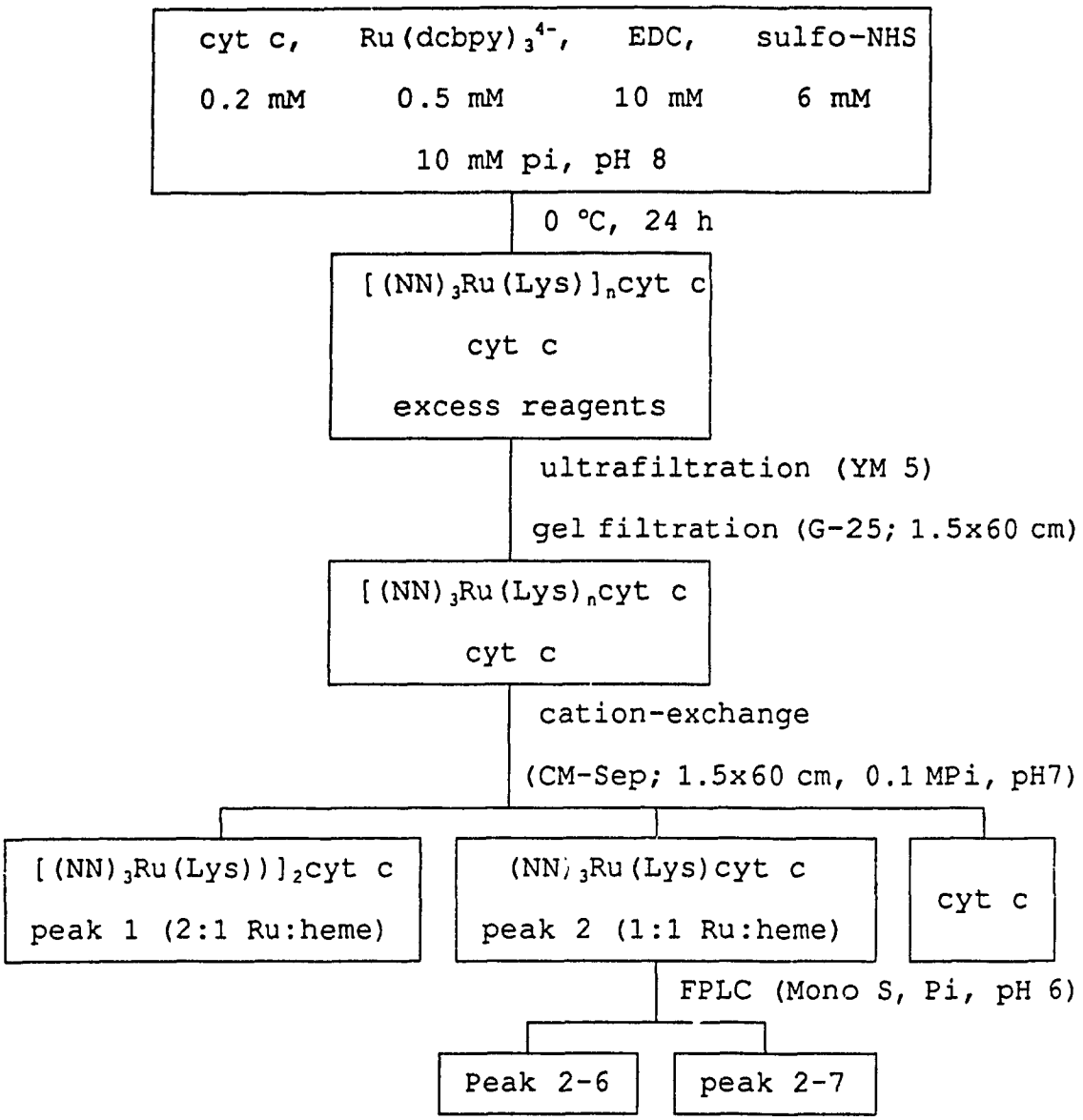

Fig.21 Flow chart for preparation and purification of $(NN)_3Ru(Lys)$cyt c

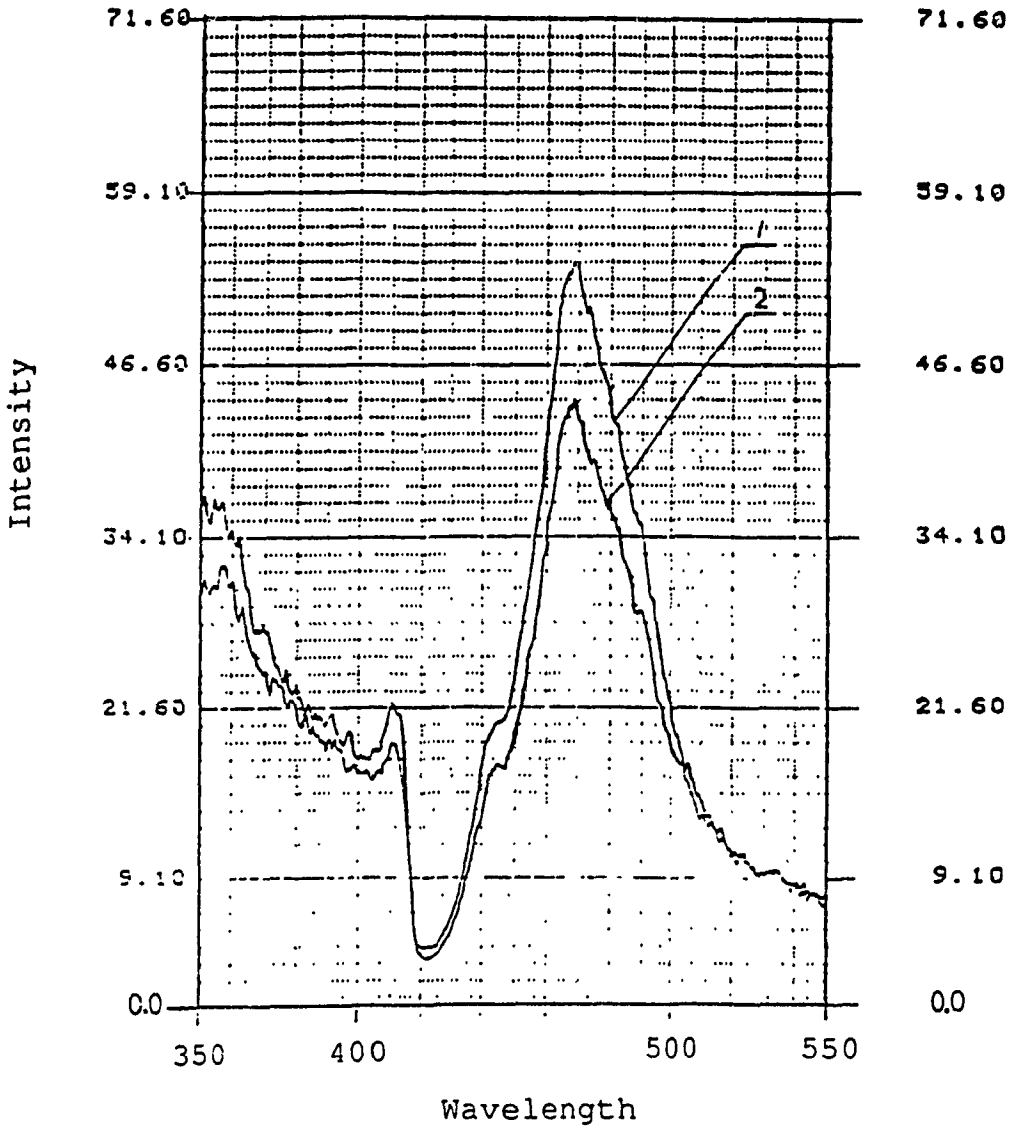

Fig.22. Excitation spectra of $(NN)_3Ru(Lys)$cyt c species in 100 mM Pi, pH 7, 20 °C. Emission wavelength, 605 nm; excitation and emission bandwidth, 10 nm; sensitivity, high; response, auto; scan speed, 60 nm/sec; (1) Peak 2-6 from Fig.17; (2) Peak 2-7 from Fig.17

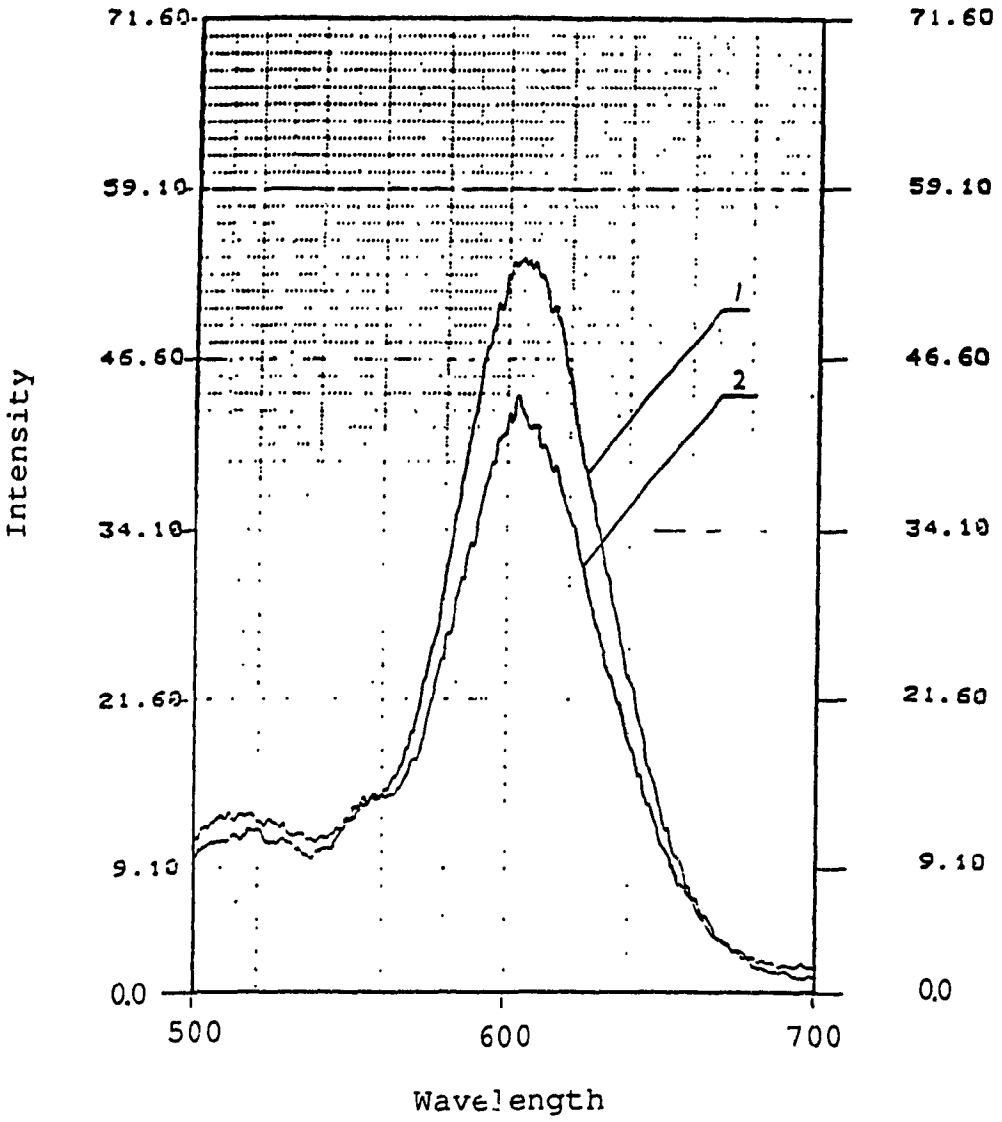

Fig.23. Emission spectra of $(NN)_3Ru(Lys)$cyt c species in 100 mM Pi, pH 7, 20 °C. Excitation wavelength, 466 nm; the other experimental conditions are given in the caption to Fig.22. (1) Peak 2-6 from Fig.17; (2) Peak 2-7 from Fig.17

Table 6: Emission intensities at 605 nm and excited-state quenching rate constants (k_q)

sample[a]	Intensity (I)[b]	I/I_o	$k_q x10^{-6}$ (s^{-1})[c] τ_o(air)=412 ns[d]
$Ru(dcbpy)_3^{4-}$	139 (I_o)	1.00	---
$Ru(dcbpy)_3^{4-}$ [e]	141	1.01	---
$Ru(dcbpy)_3^{4-}$ [f]	129	0.93	---
$(NN)_3Ru$(Lys)lysozyme	137	0.99	---
peak 1 (Fig.13)	46	0.33	4.9
peak 2 (Fig.13)	38	0.27	6.6
peak 2-2 (Fig.17)	35	0.25	7.3
peak 2-3 (Fig.17)	28	0.20	9.7
peak 2-4 (Fig.17)	38	0.27	6.6
peak 2-5 (Fig.17)	29	0.21	9.1
peak 2-6 (Fig.17)	43	0.31	5.4
peak 2-7 (Fig.17)	54	0.39	3.8
peak 2-8 (Fig.17)	28	0.20	9.7
peak 2-9 (Fig.17)	20	0.14	15
peak 2-10 (Fig.17)	35	0.25	7.3
>peak 2-10 (Fig.17)	26	0.19	10

[a] Samples in 100 mM Pi, pH 7, 20 °C, air-saturated solutions
[b] $A_{466} = 0.048$ and $\lambda_{ex} = 466$ nm
[c] k_q was estimated assuming $\tau/\tau_o = I/I_o$
[d] τ_o (air) is the estimated lifetime for $Ru(dcbpy)_3^{4-}$ in air-saturated solution (see text).
[e] In the presence of 2 μM cyt c
[f] In the presence of 2 μM cyt c in 10 mM Pi, pH 7

triplet state at 605 nm, respectively. Table 6 gives the intensities at emission maximum for the various samples. The emission intensities of $Ru(dcbpy)_3^{4-}$ and the noncovalent mixture of $Ru(dcbpy)_3^{4-}$ and cyt c, as well as the $(NN)_3Ru(Lys)$lysozyme species from the G-25 column are nearly identical, but the covalent $[(NN)_3Ru(Lys)]_2$cyt c derivatives show much lower emission intensities than the other $Ru(dcbpy)_3^{4-}$ samples. This indicates that $Ru(dcbpy)_3^{4-}$ is covalently bound to cyt c since intramolecular quenching by the heme would decrease the emission intensity of the Ru complex.

The variation in the emission intensities of the $(NN)_3Ru(Lys)$cyt c derivatives indicates that $Ru(dcbpy)_3^{4-}$ is attached to different lysines of cyt c. Different binding sites have different environments and their distances from the heme vary, resulting in a range of quenching rates. An emission lifetime (τ_o) for free $Ru(dcbpy)_3^{4-}$ of 700 ns in N_2 was reported [33]. For $Ru(bpy)_3^{2+}$, the τ_o (N_2) and τ_o (air) are 640 and 370 ns [17], respectively; thus, τ_o (N_2)/τ_o (air) = 1.7. Assuming the same ratio for $Ru(dcbpy)_3^{4-}$, gives a τ_o (air) of 412 ns. An excited-state quenching rate constant, k_q, can be estimated assuming $\tau/\tau_o = k_o/(k_o+k_q) = I/I_o$, where τ and τ_o are the emission lifetimes of $(NN)_3Ru(Lys)$cyt c and free $Ru(dcbpy)_3^{4-}$, respectively, I and I_o are the corresponding emission intensities, and $k_o = 1/\tau_o$ is the decay rate constant for the excited-state of free $Ru(dcbpy)_3^{4-}$. The k_q values estimated for the different $(NN)_3Ru(Lys)$cyt c derivatives are given in Table 6.

3.8. Analysis of tryptic digests of cyt c and $(NN)_3Ru(Lys)$cyt c by FPLC

The site of attachment of $Ru(dcbpy)_3^{4-}$ to cyt c can be identified by locating and isolating the $Ru(dcbpy)_3^{4-}$-containing tryptic peptide. When cyt c is digested with trypsin, the peptide bonds adjacent to lysine residues are cleaved. The peptide bond adjacent to a modified lysine will not be hydrolyzed during a tryptic digest, and the peak corresponding to the modified peptide will shift from its original position in the native cyt c chromatogram [35]. The modified peptide can then be identified by amino acid analysis.

Fig.24 and Fig.25 show the chromatograms of digested native cyt c from the FPLC PepRPC HR5/5 column. The samples were digested in 0.2 M NH_4HCO_3, pH 8.0 with a trypsin-to-sample ratio of 1:20 (w/w) at 37 °C for 20 h. The digestion solution (pH 8.0) was injected into the FPLC column equilibrated with 0.1% TFA (pH 2.5). TFA was used to adjust the pH of the eluant to <3, and to form ion pairs with the peptides to improve the separation [36, 37]. The CH_3CN gradient shown in Fig.24A gives a better separation than the CH_3OH gradient shown in Fig.25, so CH_3CN gradients were used to separate the tryptic peptides. However, incomplete digestion of the peptides is apparent from Fig.24. First, its absorption spectrum shows that peak 16 contains undigested cyt c, and second, the intensity of peak 5 (Lys + T8, Table 7) is higher than that of peak 6 (T8, Table 7). But it was observed that if the digestion time is increased to 40 h, the intensity of peak 5 is lower than that of peak 6, and the intensities of peaks 14 (T10 + T11 +

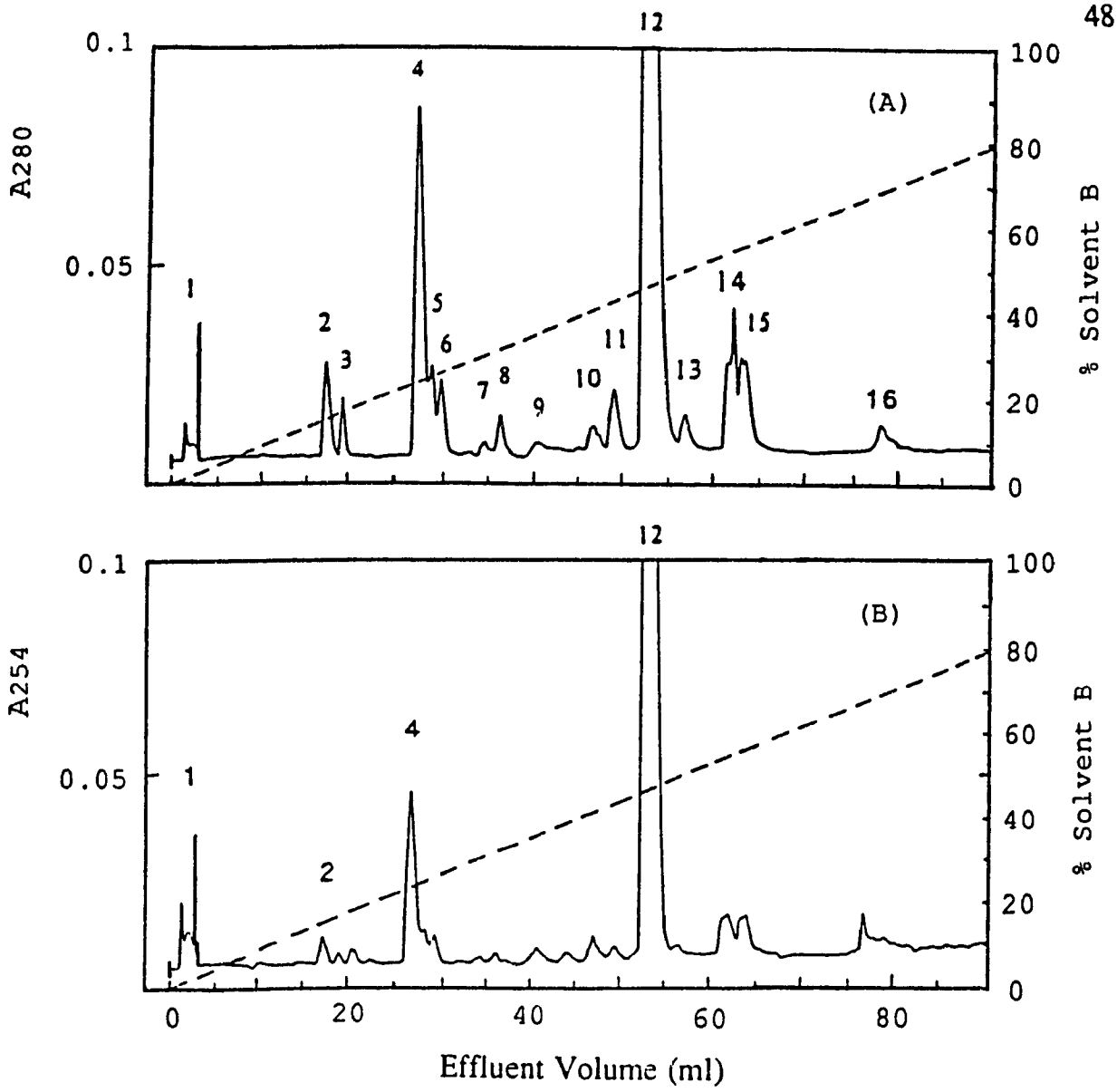

Fig.24. FPLC chromatograms of tryptic digested native cyt c. Column: PepRPC HR5/5; eluant: solvent A, 0.1% TFA in water, pH 2.5, solvent B, 0.1% TFA + 50% CH_3CN in water, pH 2.5; linear gradient 0-78.8% B in 90 ml effluent volume (dash line indicates the gradient); flow rate, 0.8 ml/min; chart speed, 0.4 cm/ml; fraction size, 0.5 ml. The FPLC program is given in Appendix 4. The column was equilibrated with solvent A, and the effluent absorbance was monitored at (A) 280 nm, and (B) 254 nm.

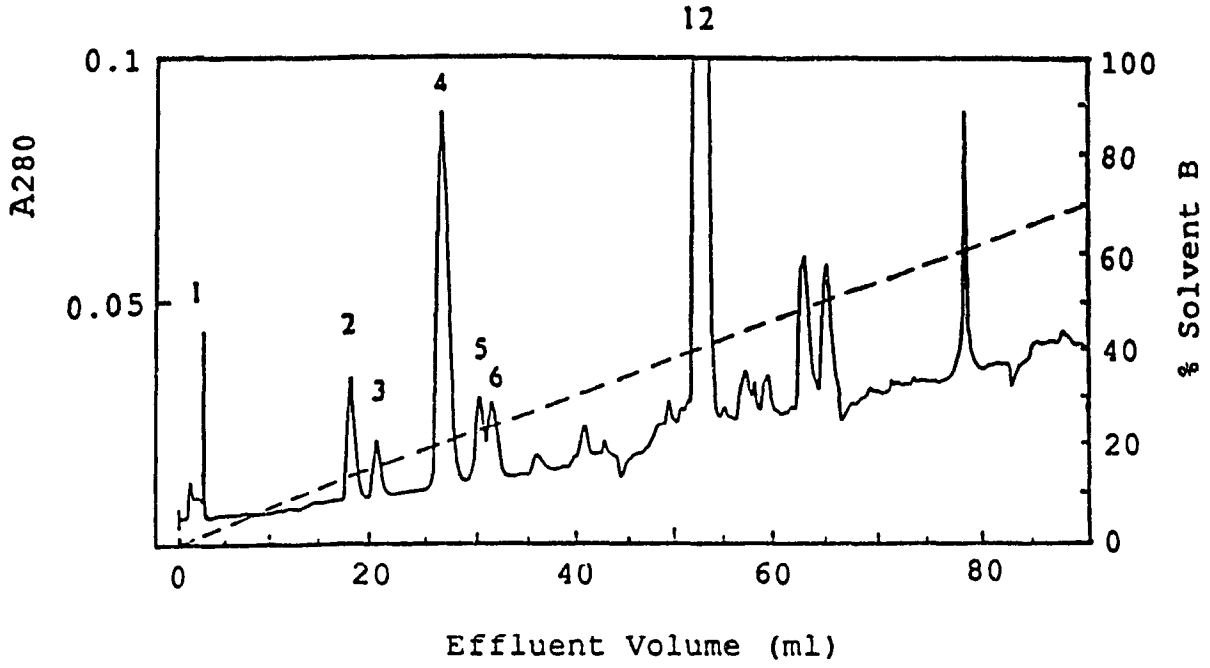

Fig.25. FPLC chromatograms of tryptic digested native cyt c. Experimental conditions as given in the caption to Fig.24 (A) except solvent B was 0.1% TFA in 100% CH_3OH. The FPLC program is given in Appendix 5.

Table 7: Identification of cyt c tryptic fragments

Fragment [a]	Tryptic peptides [b]
1[c]	T2, T5, T6, T9, T14, T17, T18
2[c]	T12
3	T3
4[c]	T10
5	Lys +T8
6	T8
7	
8[c]	T16
9	T13
10	
11	
12[c]	T4
13	T11
14	T10+T11+Lys
15	T10+T11

[a] The fragments were separated under the conditions given in Fig.26A. The fragment numbers correspond to the peak numbers in Fig.26A

[b] The amino acid sequences of the tryptic peptides are given in Fig.28.

[c] Identified at BRI. The other fragments were identified by comparison with Ref.34.

Lys, Table 7) and 15 (T10 + T11, Table 7) decrease relative to that of peak 4 (T10, Table 7) (see Fig.26). Hence, the digestion time of the samples was increased to 40 h.

Fig.26 compares the chromatograms of digested native cyt c, and those of peaks 2-6 and 2-7. The chromatogram in Fig.26A for native cyt c is similar to that obtained by HPLC [34] but some peptide bands are missing because our c ›matogram was monitored at 280 nm, where only peptides containing tyrosine, tryptophan, and phenylalanine can be detected [38]. In Figs.26B and 26C, the positions of the numbered bands are the same as in Fig.26A, but several extra Ru-containing peaks, labelled a, b, c, etc., were identified by their absorbance spectra. For comparison, $Ru(dcbpy)_3^{4-}$ alone, and a 1:1 noncovalent mixture of $Ru(dcbpy)_3^{4-}$ and cyt c were digested and eluted under the same conditions as in Fig.26, and the FPLC profiles are shown in Figs.27A and 27B, respectively. We were surprised to find three Ru peaks (labelled a, b, c) in Fig.27A, and these peaks appear at the same positions in Fig.27B. The other peak positions in Fig.27B are the same as Fig.26A. Thus, it appears that there are at least three different species in the G-25 purified $Ru(dcbpy)_3^{4-}$. Peaks 2, 4, 8, 12 in Fig.26A, peaks a, c, d, e in Fig.26B, peaks a, b, e, f in Fig.26C, and peaks a, b, c in Figs. 27A and 27B were collected and sent to the Biotechnology Research Institute (BRI) for amino acid analysis.

3.9. Amino acid analyses

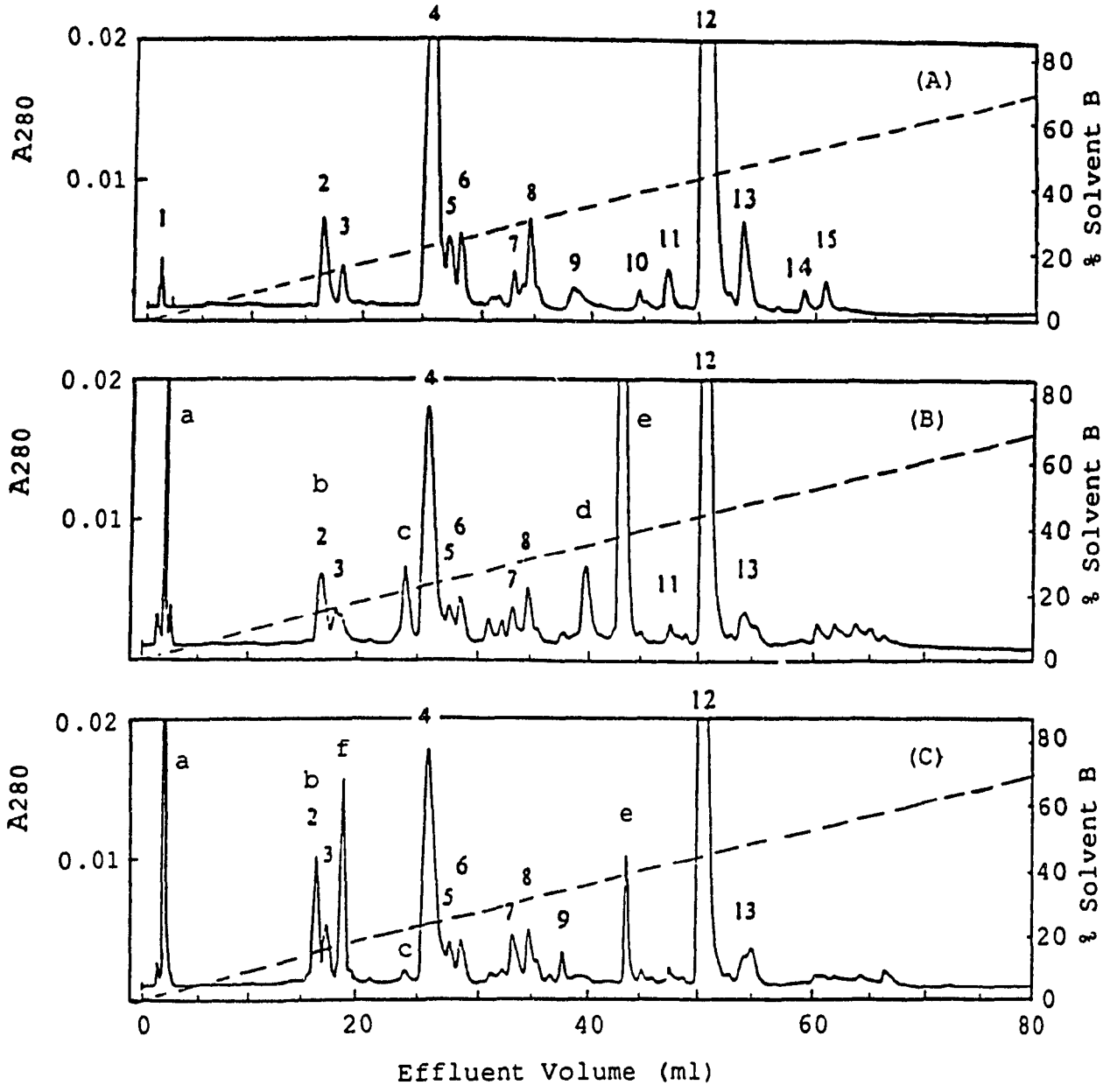

Fig.26. FPLC chromatograms of tryptic native cyt c, peaks 2-6 and 2-7 (Fig.20). Experimental conditions as given in the caption to Fig.24 (A) except the linear gradient was 0-70% B in 80 ml effluent volume; chart speed, 0.8 cm/ml; and absorbance scale was 0.02. The FPLC program is given in Appendix 6. (A). Native cyt c; (B). Peak 2-6; (C). Peak 2-7

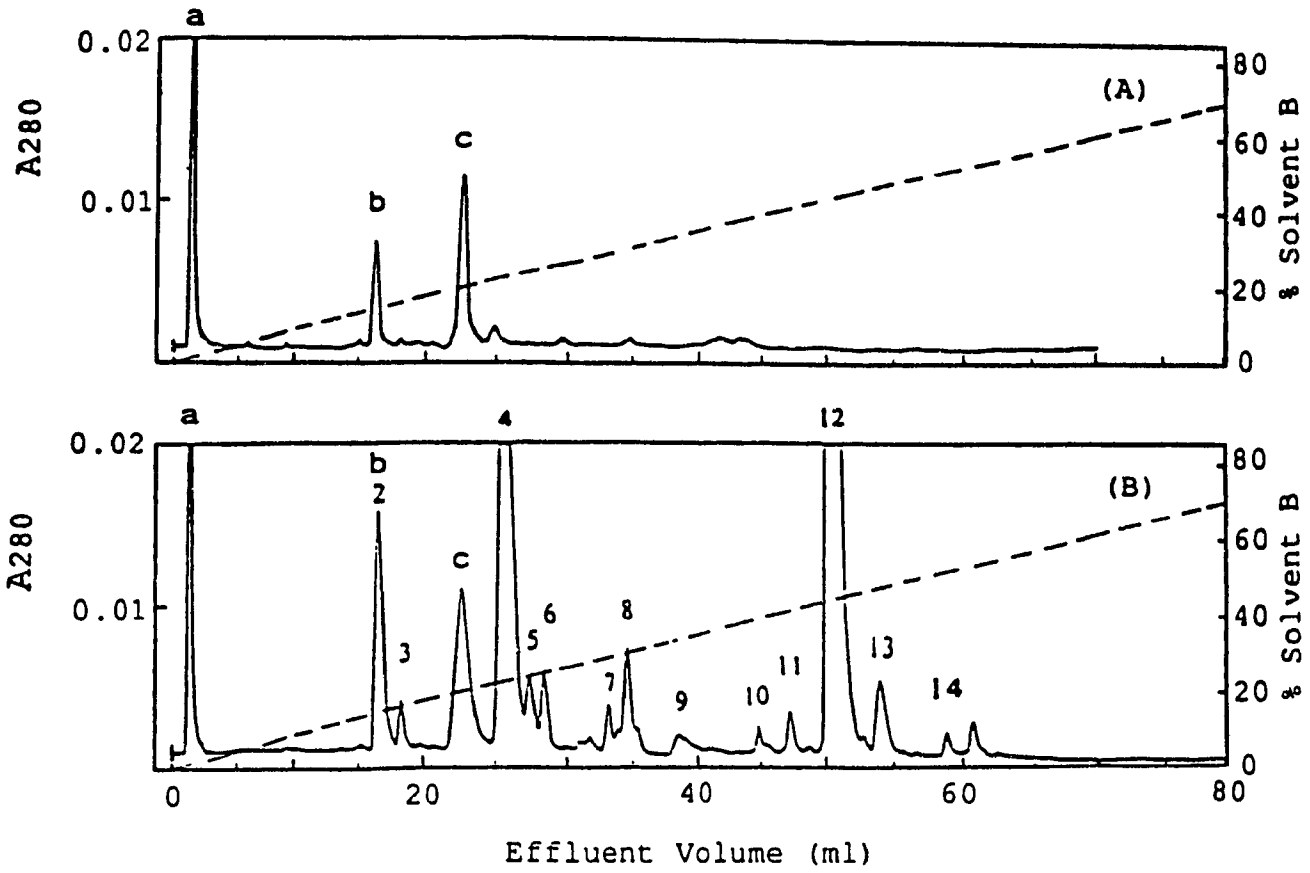

Fig.27. FPLC chromatograms of tryptic $Ru(dcbpy)_3^{4-}$, and a 1:1 noncovalent mixture of $Ru(dcbpy)_3^{4-}$ and cyt c. Experimental conditions were the same as in Fig.26. (A) $Ru(dcbpy)_3^{4-}$ alone; (B) Noncovalent mixture of $Ru(dcbpy)_3^{4-}$ and cyt c

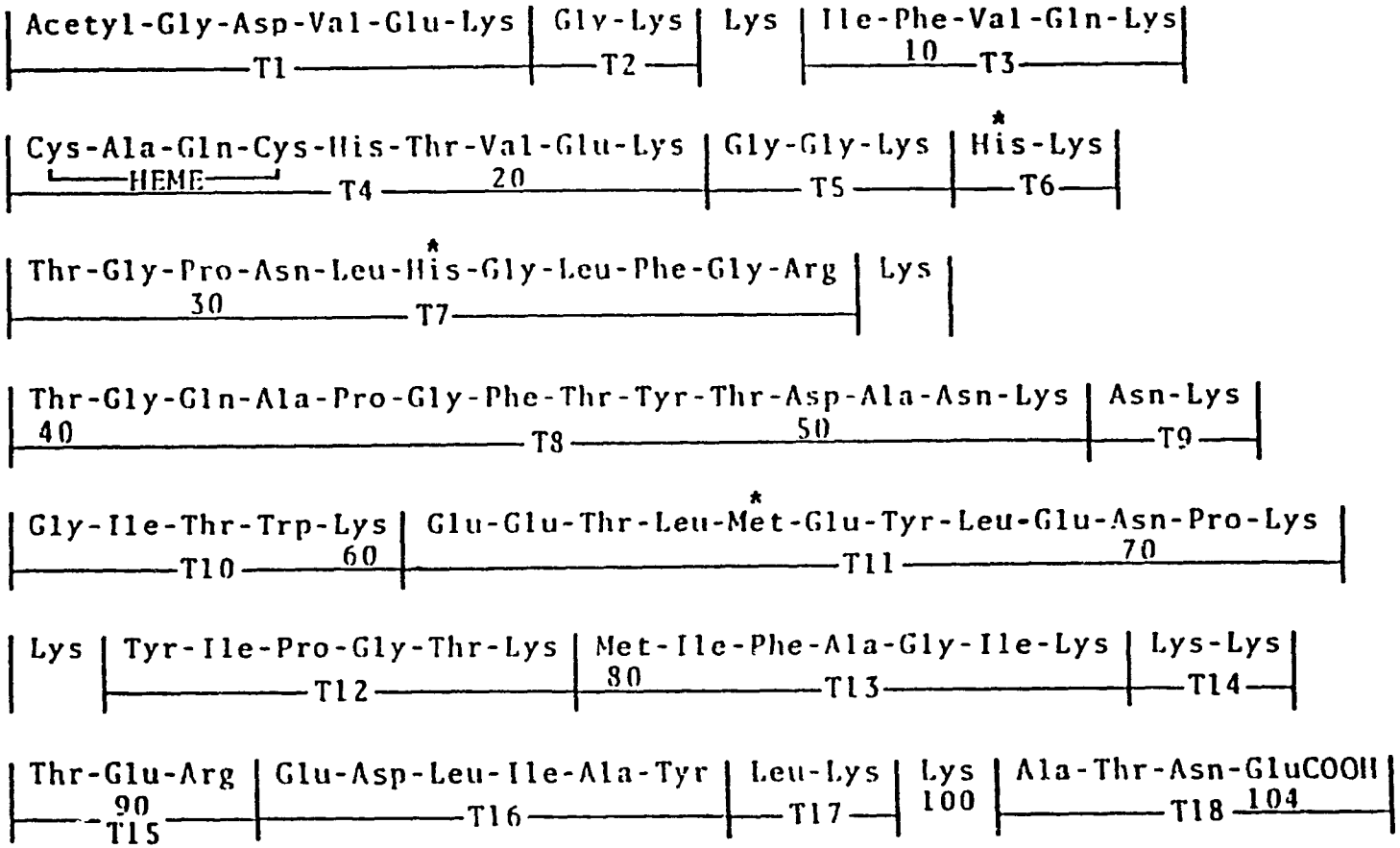

Fig.28. The tryptic peptides of native cyt c (adopted from Ref.39, p165)

The peptides expected from a tryptic digest of native cyt c are given in Fig.28 [39]. The peaks of digest native cyt c in Fig.26A were compared with Ref.32, and our assignment is given in Table 7. The amino acid analyses of the tryptic fragments of native cyt c, (Fig.26A), $Ru(dcbpy)_3^{4-}$ alone (Fig.27A), and the noncovalent mixture of $Ru(dcbpy)_3^{4-}$ and cyt c (Fig.27B) were carried out at BRI, and the results are given in Tables 8, 9 and 10. Fragments of native cyt c were identified without much difficulty. The fragments corresponding to native cyt c in the mixture of $Ru(dcbpy)_3^{4-}$ and cyt c were also identified but with some interferences, and some amino acids were detected in the fragments of $Ru(dcbpy)_3^{4-}$ alone (Table 9), indicating contamination.

The Ru-containing fragments of peak 2-6 (Fig.26B), peak 2-7 (Fig.26C) were also analyzed at BRI, and the results are given in Tables 11 and 12. The results indicate that the Ru-containing peptides are also contaminated. For example, there is no serine in cyt c, but Tables 11 and 12 show that the peptides contain 2-20% serine. Where does the interference come from? Amino acid analyses at BRI of native cyt c and undigested peak 2-7 showed the expected values. Therefore, it is possible that the interference comes from hydrolysis products of trypsin. Autolysis of trypsin on prolonged digestion will produce a large number of peptides which can interfere with amino acid analyses [34, 40]. Fig.29 shows the amino acid sequence of bovine trypsin [41, 42]. Its amino acid composition is:

Ala 14	Arg 2	Asp 5	Asn 17	Cys 12
Glu 2	Gln 12	Gly 25	His 3	Ile 15
Leu 14	Lys 14	Met 2	Phe 3	Pro 8
Ser 34	Thr 10	Trp 4	Tyr 10	Val 17

There are 34 serines which are the most likely source of serine in Tables 11 and 12. Small peptides from the hydrolysis product of trypsin with different retention times may appear at different positions and overlap with the peptides from the samples. Since many amino acids were detected in the tryptic fragments of $Ru(dcbpy)_3^{4-}$ (Table 9), these must arise from the hydrolysis products of trypsin. Thus, the serious contamination of fragments d and e in Fig.26B and fragments f and e in Fig.26C probably results mainly from these small peptides. Unfortunately, it is not possible to detect all the interfering peptides at 280 nm, only those that contain tyrosine, tryptophen or phenylalanine. A 214 nm monitor (Zn lamp) would detect all the peptides but we do not have one.

3.10. Identification of Ru-containing peptides

There are five Ru-containing peaks in Fig.26B (peak 2-6), and Fig.26C (peak 2-7). Peaks a, b and c in both Figs.26B and 26C are probably due to mixtures of free $Ru(dcbpy)_3^{4-}$ and native cyt c peptides, since their positions are the same as peaks a, b and c in Fig.27. These peaks must arise from cleavage of the

Table 8: AA analysis of tryptic fragments of cyt c in Fig.26A[a,b]

AA	Fragment 2		Fragment 4		Fragment 8		Fragment 12	
	nM[c]	%mole	nM[c]	%mole	nM[c]	%mole	nM[c]	%mole
Asp					0.97	15	0.05	0.70
Thr	0.25	17	0.21	20	0.07	1.1	0.86	11
Ser	0.06	4.2	0.03	2.7	0.14	2.2	0.09	1.2
Glu	0.05	3.2			1.2	18	2.1	27
Gly	0.33	22	0.29	27	0.20	3.2	0.10	1.3
Ala					0.97	15	0.99	13
Cys							0.53	7.0
Val							0.96	13
Met					0.15	2.4		
Ile	0.27	18	0.24	23	0.98	15		
Leu					0.90	14		
Tyr	0.24	16			0.69	11		
Phe					0.20	3.1		
His					0.02	0.30	0.96	13
Lys	0.28	19	0.28	27	0.03	0.50	0.98	13
Arg								
Trp								
Assign.[d]	T12		T10		T16		T4	

[a] Sample was digested with trypsin in 0.2 M NH_4HCO_3 (pH 8) at 37 °C for 40 h with a trypsin-to-sample ratio of 1 to 20 (w/w), 0.2 mg sample was injected into FPLC PepRPC column.

[b] Data were obtained at BRI by B. Gibbs.

[c] Concentration in nM

[d] Assignment of fragments to tryptic peptides in Table 7

Table 9: AA analysis of tryptic fragments of $Ru(dcbpy)_3^{4-}$ in Fig.27A[a,b]

AA	Fragment a		Fragment b		Fragment c	
	nM[c]	%mole	nM[c]	%mole	nM[c]	%mole
Asp	0.14	14	0.07	8.4	0.17	10
The	0.09	8.9	0.03	3.8	0.09	5.3
Ser	0.17	17	0.19	25	0.36	21
Glu	0.16	16	0.19	24	0.32	19
Gly	0.23	23	0.22	29	0.41	24
Ala	0.10	9.9			0.14	8.3
Cys						
Val						
Met						
Ile			0.06	7.1	0.05	2.7
Leu					0.09	5.2
Tyr						
Phe						
His			0.03	3.2	0.05	2.9
Lys	0.12	12			0.03	1.6
Arg						

[a, b, c] See footnotes to Table 8.

Table 10: AA analysis of tryptic fragments of 1:1 noncovalent mixture of $Ru(dcbpy)_3^{4-}$ and cyt c in Fig.27B[a,b]

AA	Frag.a nM[c]	Frag.b nM[c]	Frag.c nM[c]	Frag.4 nM[c]	Frag.8 nM[c]	Frag.12 nM[c]
Asp	1.8	0.15	0.08	0.12	0.53	0.18
Thr	1.1	0.15	0.04	0.44	0.17	0.61
Ser	0.15	0.35	0.14	0.24	0.28	0.37
Glu	1.2	0.30	0.13	0.24	1.0	1.6
Gly	1.2	0.48	0.14	0.76	0.36	0.49
Ala	1.0	0.12	0.07	0.09	0.55	0.70
Cys						0.48
Val						0.63
Met				0.06	0.33	0.02
Ile		0.14		0.51	0.67	0.05
Leu		0.08		0.08	0.61	0.16
Tyr					0.46	
Phe					0.26	
His		0.06	0.03	0.04	0.04	0.67
Lys	2.9	0.10	0.02	0.50	0.08	0.67
Arg	0.26					
Assign.[d]				T10	T16	T4

[a, b, c, d] See footnotes to Table 8.

Table 11: AA analysis of Ru-containing tryptic fragments of peak 2-6 in Fig.26B[a,b,c]

AA	Fragment a		Fragment b		Fragment d		Fragment e	
	nM[c]	%mole	nM[c]	%mole	nM[c]	%mole	nM[c]	%mole
Asp	1.4	19	0.16	7.0	0.13	6.8	0.30	5.5
Thr	0.68	9.3	0.09	3.9	0.06	3.4	0.18	3.3
Ser	0.28	3.8	0.37	16	0.26	14	0.61	12
Glu	1.2	16	0.26	11	0.19	10	0.55	10
Gly	0.84	12	0.48	20	0.38	20	0.94	18
Ala	0.41	5.6	0.29	12	0.19	11	0.63	12
Val	0.49	6.7	0.11	4.7	0.08	4.5	0.15	2.8
Met	0.02	0.24	0.01	0.29	0.03	1.8	0.24	4.5
Ile	0.08	1.0	0.11	4.6	0.11	5.8	0.43	8.0
Leu	0.15	2.0	0.06	2.6	0.08	4.3	0.17	3.2
Tyr	0.04	0.56	0.04	1.5	0.01	0.72	0.06	1.2
Phe	0.04	0.57	0.04	1.7	0.09	4.6	0.35	6.5
His	0.02	0.31	0.06	2.7	0.05	2.8	0.11	2.0
Lys	1.2	16	0.20	8.4	0.11	5.7	0.49	9.1
Arg	0.22	3.0	--	--	0.02	1.2	0.04	0.68
Pro	0.33	4.5	0.07	2.8	0.06	2.9	0.12	2.2

[a,b,c] See footnotes to Table 8.

Table 12: AA analysis of Ru-containing tryptic fragments of peak 2-7 in Fig.26C[a,b]

AA	Fragment a		Fragment b		Fragment f		Fragment e	
	nM[c]	%mole	nM[c]	%mole	nM[c]	%mole	nM[c]	%mole
Asp	2.0	15	0.24	8.5	0.15	6.1	0.15	8.2
Thr	0.95	6.8	0.12	4.4	0.20	8.2	0.07	3.6
Ser	0.26	1.9	0.56	20	0.37	16	0.28	15
Glu	2.0	14	0.39	14	0.32	14	0.24	13
Gly	2.9	21	0.56	18	0.40	17	0.34	19
Ala	0.82	5.9	0.17	6.1	0.13	5.4	0.17	9.5
Val	0.74	5.3	0.16	5.7	0.10	4.1	0.09	4.7
Met	0.02	0.17	0.01	0.42	0.01	0.23	0.03	1.8
Ile	0.11	0.81	0.06	2.2	0.09	4.0	0.08	4.6
Leu	0.18	1.3	0.10	3.4	0.06	2.5	0.08	4.1
Tyr	0.06	0.39	0.05	1.8	0.06	2.7	0.03	1.8
Phe	0.05	0.38	0.03	1.0	0.03	1.1	0.10	5.5
His	0.03	0.19	0.11	3.8	0.06	2.5	0.05	2.4
Lys	3.2	23	0.12	4.2	0.16	6.5	0.06	3.2
Arg	0.40	2.8	0.03	1.0	0.12	5.2	---	---
Pro	0.29	2.1	0.18	5.7	0.13	5.4	0.07	3.5

[a,b,c] See footnotes to Table 8.

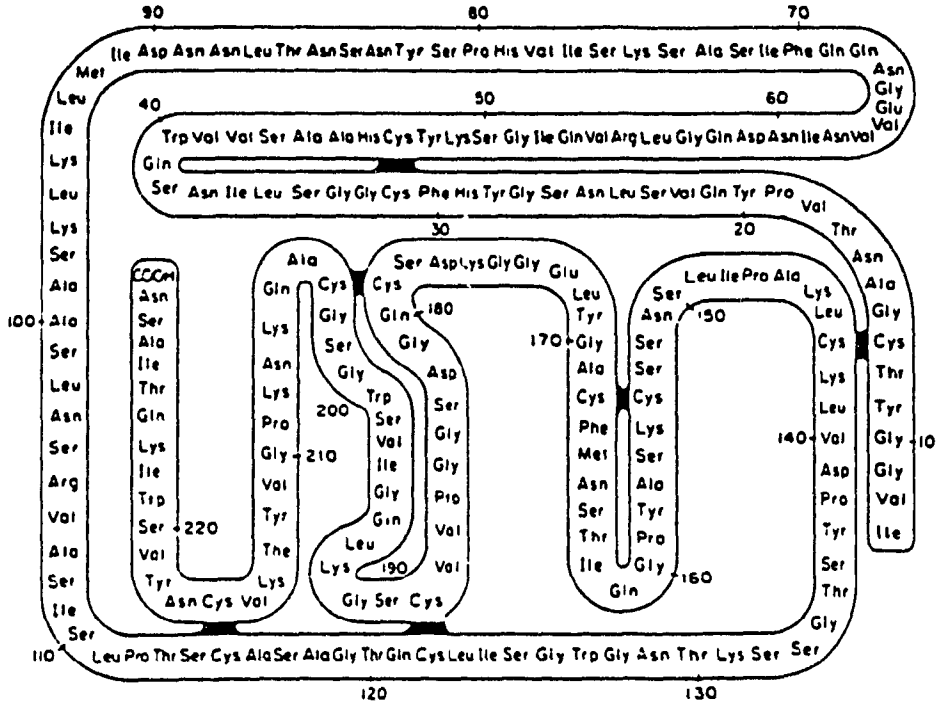

Fig.29. Primary structure of bovine trypsin (adopted from Ref.42)

bond between the Ru complex and cyt c in $(NN)_3Ru(Lys)$cyt c during tryptic digestion. Long digestion times decrease the intensities of Ru-labelled peptides since after loss of Ru a peptide elutes at its original position.

Peaks d and e in Fig.26B and peaks e and f in Fig.26C do not appear in Fig.27. Hence, these peaks probably contain covalently-bound Ru. An examination of Figs.26B and 26C shows that peak e is much more abundant in the former. Hence, the mole fraction (mole%) of contaminating amino acids should be less for fragment e in Table 11 compared to Table 12. This is case for all the amino acids except the following: Ala, Met, Ile, Phe, Lys and Gly, which corresponds to peptide T13 (Fig.28), and indicates that Lys 86 may be the attachment site in peak 2-6 (Fig.17).

The lysines mainly modified by $Ru(bpy)_2(dcbpy)$ are 86, 87, 72, 8, 13, 25, 27 [27, 28]. Although there are serious interferences, not much Met is present in the samples in Tables 8-12. There are only two Met-containing residues in trypsin, so that the interference of Met from trypsin should be small. Fragments e and d of peak 2-6 (Fig.26B) contain 4.51% and 1.83% Met respectively, which probably comes from a cyt c peptide. There are only two cyt c peptides that contain Met, T11 and T13 (Fig.28); thus, both Lys 72 of T11 or Lys 86 of T13 may be the Ru attachment sites in peak 2-6. If Lys 86 is the modified residue, fragment e would be:

$$\overset{80}{\text{Met-Ile-Phe-Ala-Gly-Ile-}}\overset{86}{\text{Lys}}\overset{87}{\text{-Lys}} \qquad \text{(I)}$$

$$\Big|$$

$$\text{Ru(dcbpy)}_3^{4-}$$

If Lys 72 is the modified residue, fragment e would be:

$$\overset{61}{\text{Glu-Glu-Thr-Leu-Met-Glu-Tyr-Leu-Glu-Asn-Pro-}}\overset{72}{\text{Lys}}\overset{73}{\text{-Lys}} \qquad \text{(II)}$$

$$\Big|$$

$$\text{Ru(dcbpy)}_3^{4-}$$

Table 13 compares the theoretical amino acid content of peptides I and II with that observed for fragment e (Table 11). Assuming that excess amino acids are from interference, the values for fragment e are closer to those expected for peptide (I) than peptide (II). Peak d in Fig.26B may be also due to modification at Lys 86, but arise due to loss of Lys 87. Alternatively, peak e may also contain Lys 88 and peak d would then correspond to peptide I above.

Met was detected (Table 12) in peak e of Fig.26C so that both Lys 72 and Lys 87 are possible modification positions. However, peak e has the same position in Figs.26B and 26C, which implies that in both cases this peak arises from similar peptides. Therefore, the cyt c derivative in peak 2-7 may be modified at Lys 87. Tryptic cleavage of this derivative would give rise to a peptide with the following structure:

$$\overset{80}{\text{Met-Ile-Phe-Ala-Gly-Ile-Lys-}}\overset{86}{\text{Lys}}\overset{87}{\text{-Lys}}\overset{88}{\text{-Lys}} \qquad \text{(III)}$$

$$\text{Ru(dcbpy)}_3^{4-}$$

This peptide would have a similar retention time to peptide I above if the Lys 87 - Lys 88 bond is not cleaved in the later. The retention time of peak f in Fig.26C is much shorter than that of peak e, and it contains only 0.23% Met. It is possible that the bond between Ile 85 and Lys 86 in peptide III is also cleaved during the digestion, resulting in peptide (IV) with a short retention time:

$$\overset{86}{\text{Lys}}\overset{87}{\text{-Lys}}\overset{88}{\text{-Lys}} \qquad \text{(IV)}$$

$$\text{Ru(dcbpy)}_3^{4-}$$

The amount of digested cyt c injected into the PepRPC HR5/5 column was the same in Figs.26B and 26C. Hence, all the non-Ru-containing peak intensities are the same, but the intensity of the Ru-containing peak e in Fig.26B is much stronger than that of either peak e or f in Fig.26C. This supports the assignment of the Ru-attachment site to Lys 87 since this will give rise to two Ru-containing peptides. To support the above conclusions, we repeated the digestion of peaks 2-6 and 2-7, native cyt c and noncovalent mixture of $Ru(dcbpy)_3^{4-}$ and cyt c using highly-active trypsin, under strictly controlled digestion conditions. The samples were digested at 37 °C for 15 h with a trypsin-to-protein ratio of 1:20 (w/w). The

digested samples were separated under the same conditions given in Fig.26, and the chromatograms are essentially the same as those given in Fig.26 and Fig.27B. Fragments 2, 4, 8, 12, 13, b + 2, c, d, e, f were sent to BRI for amino acid analysis. The fragments were assigned without difficulty (Table 14) because contamination was negligible (e.g. no significant Ser was detected), and the results fully support our conclusions. However, fragment e was observed to contain Peptide T7 in addition to T13 + Lys. No peak appears with the same retention time as fragment e in Fig.26A, but because peptide T7 does not contain Tyr and Trp, it was not detected by our 280 nm monitor. Secondly, fragment f was found to contain peptides T14 + T15, which means that the modification site could also be Lys 88. However, modification at Lys 88 would not give rise to a Ru-containing fragment e (T13 + Lys) in the chromatogram of peak 2-7. Also, the intensity of fragment f is much lower than that of fragment e in Fig.26B; thus, it is likely that fragments f and e in Fig.26C arise because modification at Lys 87 permits tryptic cleavage at Lys 87 but not at Lys 88. This supports the assignment of the modification site to Lys 87 in peak 2-7.

3.11. FPLC reverse phase chromatography of $Ru(dcbpy)_3^{4-}$

Only one Ru-containing peak is expected in the tryptic chromatogram of $Ru(dcbpy)_3^{4-}$ alone, and in the noncovalent mixture of $Ru(dcbpy)_3^{4-}$ and cyt c (Figs.27A, 27B). In order to check that the digestion procedure did not alter the

Table 13: Comparison of Amino Acid Content of Fragment e and Peptides I and II[a]

AA	Peptide I %mole		Peptide II %mole		Fragment e[b] %mole	
Met	12.5	(1)[c]	7.7	(1)[c]	4.5	(1)[c]
Ile	25	(2)	0		8	(2)
Phe	12.5	(1)	0		6.5	(1.5)
Ala	12.5	(1)	0		11.7	(3)
Gly	12.5	(1)	0		17.5	(4)
Lys	25	(2)	15.4	(2)	9.1	(2)
Glu			30.1	(4)	10.2	(2.3)
Thr			7.7	(1)	3.3	(0.7)
Leu			15.4	(2)	3.2	(0.7)
Tyr			7.7	(1)	1.2	(0.3)
Asn			7.7	(1)	0	
Pro			7.7	(1)	2.2	(0.5)

[a] Peptides I and II are expected on Lys 86 and Lys 72 modification, respectively (see text).

[b] Experimental values for fragment e from Table 11

[c] The values in brackets are the mole ratios assuming %mole = 1 for Met.

Table 14: Assignments of New Tryptic Fragments[a]

Fragment	Assignment
2	T12
4	T10
8	T16
12	T4
13	T11
c	T2
d	T13
e	T13 + Lys, T7
f	T14 + T15

[a] Peaks 2-6 and 2-7, native cyt c, and noncovalent mixture of cyt c and $Ru(dcbpy)_3^{4-}$ were digested at 37 °C for 15 h with a trypsin-to-protein ratio of 1:20 (w/w) using highly-active trypsin. The FPLC separation conditions were the same as Fig.26, and the chromatograms were almost the same as those in Figs.26 and 27B. The fragments were assigned at BRI by B. Gibbs.

$Ru(dcbpy)_3^{4-}$ complex, a sample purified by gel filtration (Fig.4) was applied to the FPLC PepRPC HR5/5 column and the chromatograms are shown in Fig.30. The FPLC conditions are the same as those given in Fig.27 except that samples in 0.1% TFA were injected into column. Since $Ru(dcbpy)_3^{4-}$ has low solubility at pH 2.5, the derivatives of cyt c in peaks 2-6 and 2-7 were previously injected into the FPLC column in the original digestion solution at pH 8. The pH difference between the sample (pH 8) and the column (pH 2.5) changes the retention times of Ru species in Fig.27A compared to those in Fig.30A. From Fig.30A, it can be seen that the $Ru(dcbpy)_3^{4-}$ sample gives rise to at least five different peaks on the reverse phase column. Also evident from Fig.30 is that as the solvent pH increases, the retention time and the number of bands decreases. One possibility is that these different bands may contain Ru species with different numbers of COOH groups due to decarboxylation during the preparation procedure. The FPLC chromatograms of $Ru(dcbpy)_3^{4-}$ and $Ru(bpy)_2(dcbpy)$ at pH 8.0 are given in Fig.31. There is one major band in the $Ru(bpy)_2(dcbpy)$ profile (Fig.31B) and its retention time is much longer than any of the species in Fig.31A. Thus, the retention time clearly depends on the number of COOH group present in the complex. Fig.32 shows the absorption spectra of the major peaks in Fig.31A. The ratio A_{304}/A_{466} = 3.4 at pH 8.0 for band 2 in Fig.31A is the same as that given for the $Ru(dcbpy)_3^{4-}$ sample in Table 1. Band 6, however, has a lower ratio (A_{304}/A_{466} = 3.1), suggesting that the multiple peaks observed for $Ru(dcbpy)_3^{4-}$ on reverse phase

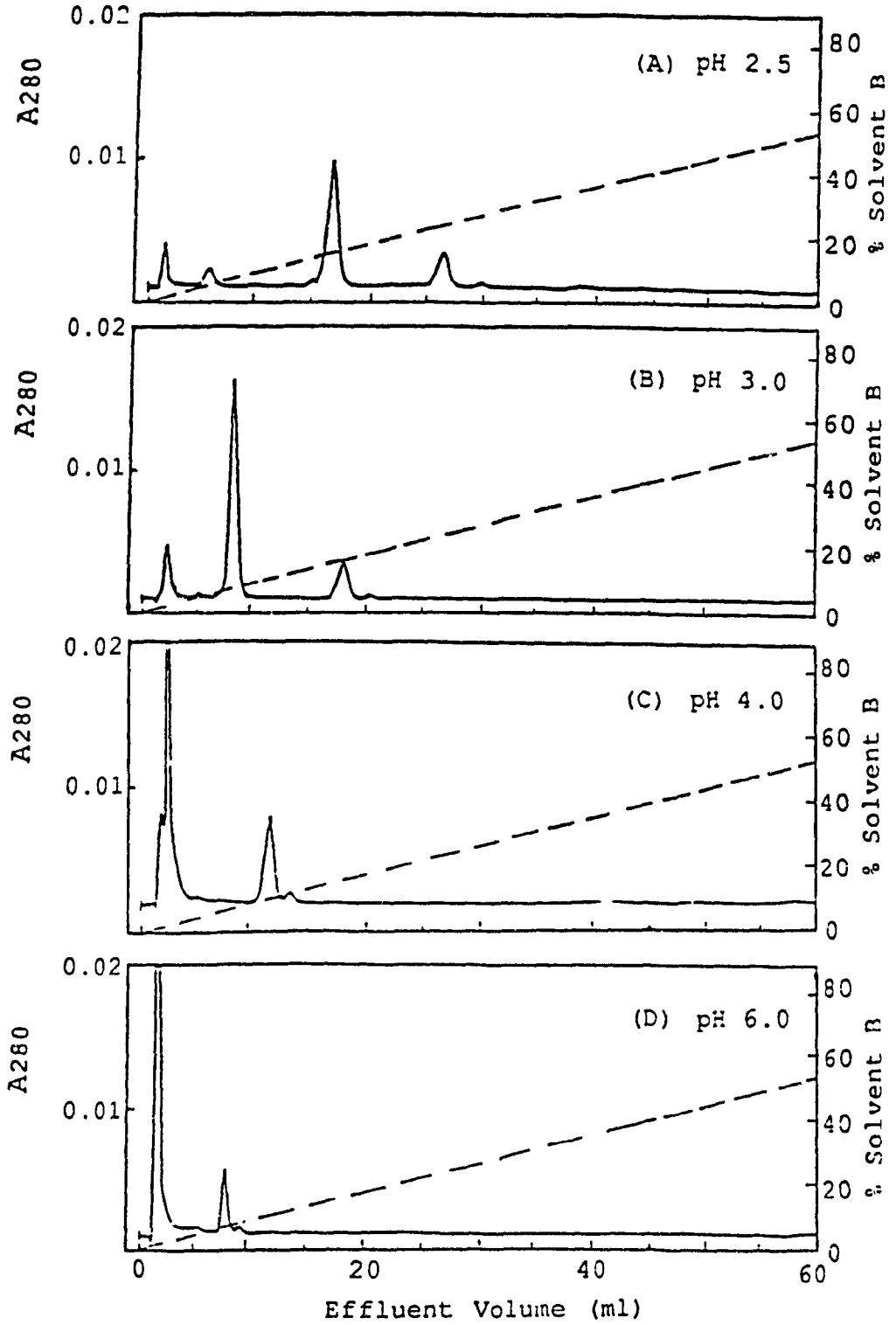

Fig.30. FPLC chromatograms of $Ru(dcbpy)_3^{4-}$ at different pH's. (A) Solvent A, 0.1% TFA in water, pH 2.5, solvent B, 0.1% TFA + 50% CH_3CN in water, pH 2.5; (B) Solvent A, 55 mM Pi, pH 3.0, solvent B, 0.1% TFA + 50% CH_3CN in 55 mM Pi, pH 3.0; (C) Solvents were the same as (B), pH 4.0; (D) Solvents were the same as (B), pH 6.0. Samples were dissolved in solvent A before applying to column, all other FPLC conditions were the same as Fig.26.

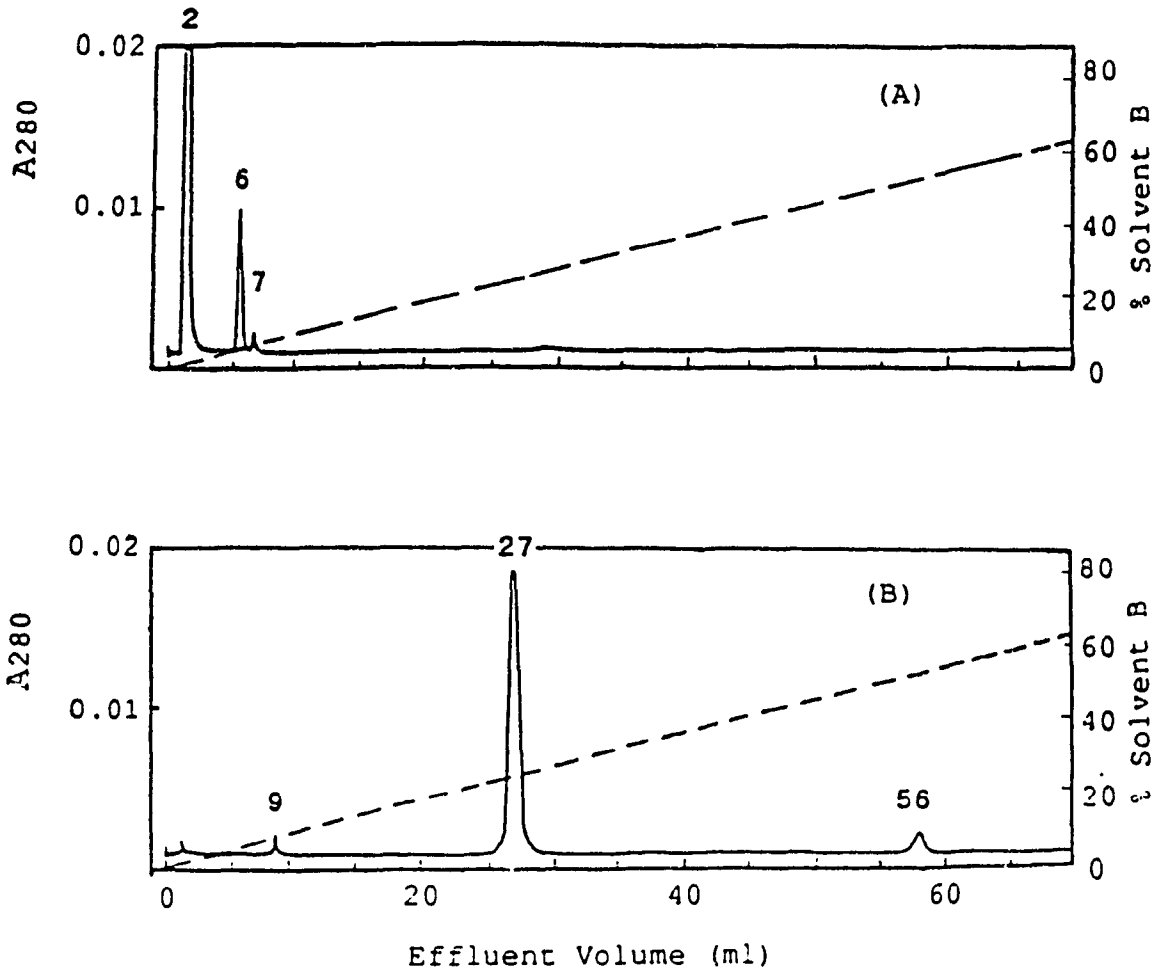

Fig.31. FPLC chromatograms of $Ru(dcbpy)_3^{4}$ and $Ru(bpy)_2(dcbpy)$. Column: PepRPC HR5/5; eluant: solvent A, 55 mM Pi, pH 8.0, solvent B, 50% A + 50% CH_3CN, pH 8.0. The absorbance scale was 0.2. The samples were injected into the column in solvent A. All other FPLC conditions were the same as Fig.26. (A) $Ru(dcbpy)_3^{4-}$; (B) $Ru(bpy)_2(dcbpy)$. Numbers on peaks indicate the effluent volumes (ml).

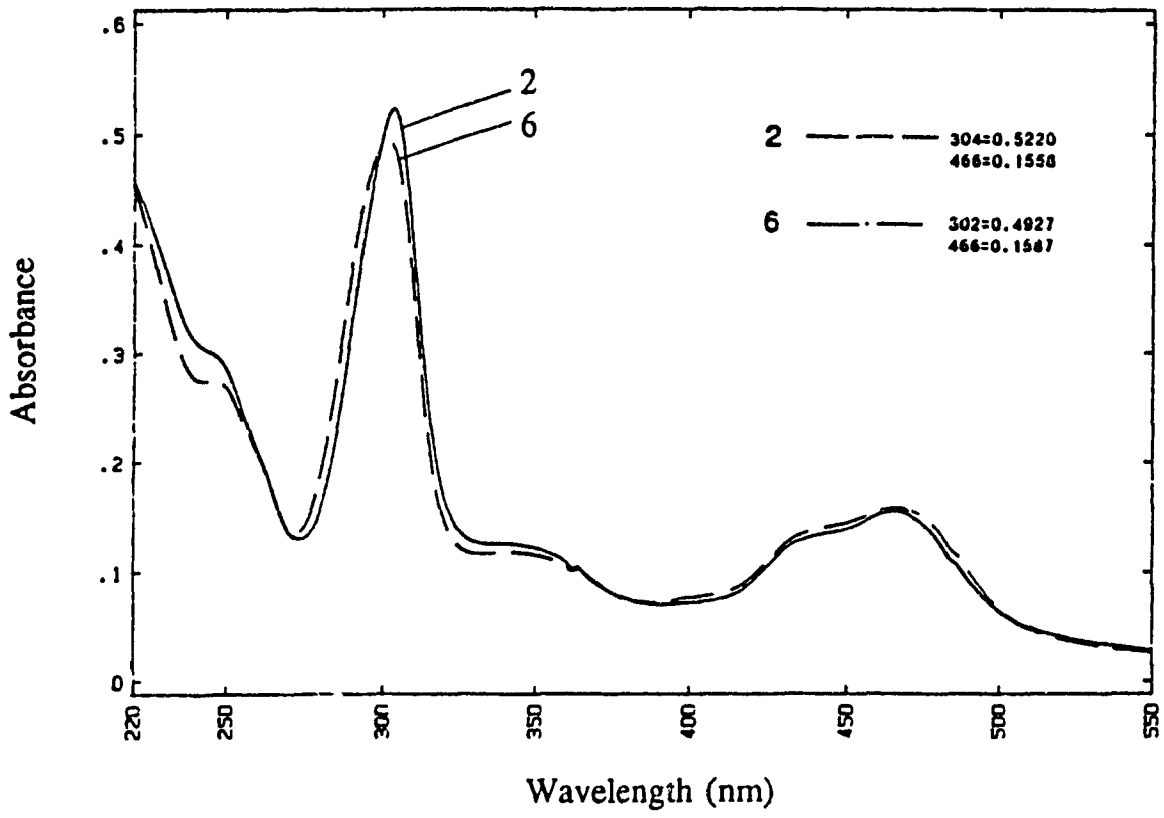

Fig.32. Absorbance spectra of Ru complexes from Fig.31A at pH 8.0. The numbers on the spectra indicate the effluent volume (ml).

column arise from at least two Ru complexes.

Dunn et al. [43, 44] reported that picolinic acid decarboxylates in aqueous solutions at 95 °C. In order to check whether dcbpy also decarboxylates, free dcbpy was refluxed at 90 °C for 24 h as in the preparation of $Ru(dcbpy)_3^{4-}$. Fig.33 compares the FPLC profiles of dcbpy that has been refluxed with untreated dcbpy and bpy from the bottle. Since bpy has a longer retention time than the carboxylated species, decarboxylation would give rise to a new peak with a longer retention time than dcbpy. There is no evidence that indicates decarboxylation of dcbpy in Fig.33, but the solubility of refluxed dcbpy is reduced, resulting in a lower absorbance in Fig.33B. Since saturated solutions of the samples were injected into the column to obtain the chromatograms in Fig.33A and 33B, this decrease in absorbance is unexpected, but it was not investigated further.

However, it is possible that $Ru(dcbpy)_3^{4-}$ undergoes decarboxylation under conditions where free dcbpy does not. Peptide analysis of peaks 2-6 and 2-7 shows the same Ru-containing peaks (a, b, c) as free $Ru(dcbpy)_3^{4}$ due to loss of $Ru(dcbpy)_3^{4-}$. But if cyt c was modified with different $Ru(dcbpy)_3^{4-}$ species, these would be readily separated by ion-exchange chromatography since this technique can separate isoelectric species based on dipole differences only. Thus, we conclude that $Ru(dcbpy)_3^{4-}$ does not behave as expected on the reverse phase column at low pH. Therefore, while G-25 purified $Ru(dcbpy)_3^{4-}$ may contain some non-isoelectric species such as $Ru(dcbpy)_2(mcbpy)^{3-}$ (where mcbpy = 4-

monocarboxy-2,2'-bipyridine), the $(NN)_3Ru(Lys)$cyt c species in peaks 2-6 and 2-7 (Fig.17) must contain cyt c derivatized with isoelectric Ru complexes. Since these peaks are the most abundant in Fig.17, we assume that they contain cyt c derivatized with $Ru(dcbpy)_3^{4-}$, which appears to be the major species in G-25 purified sample according to Fig.32.

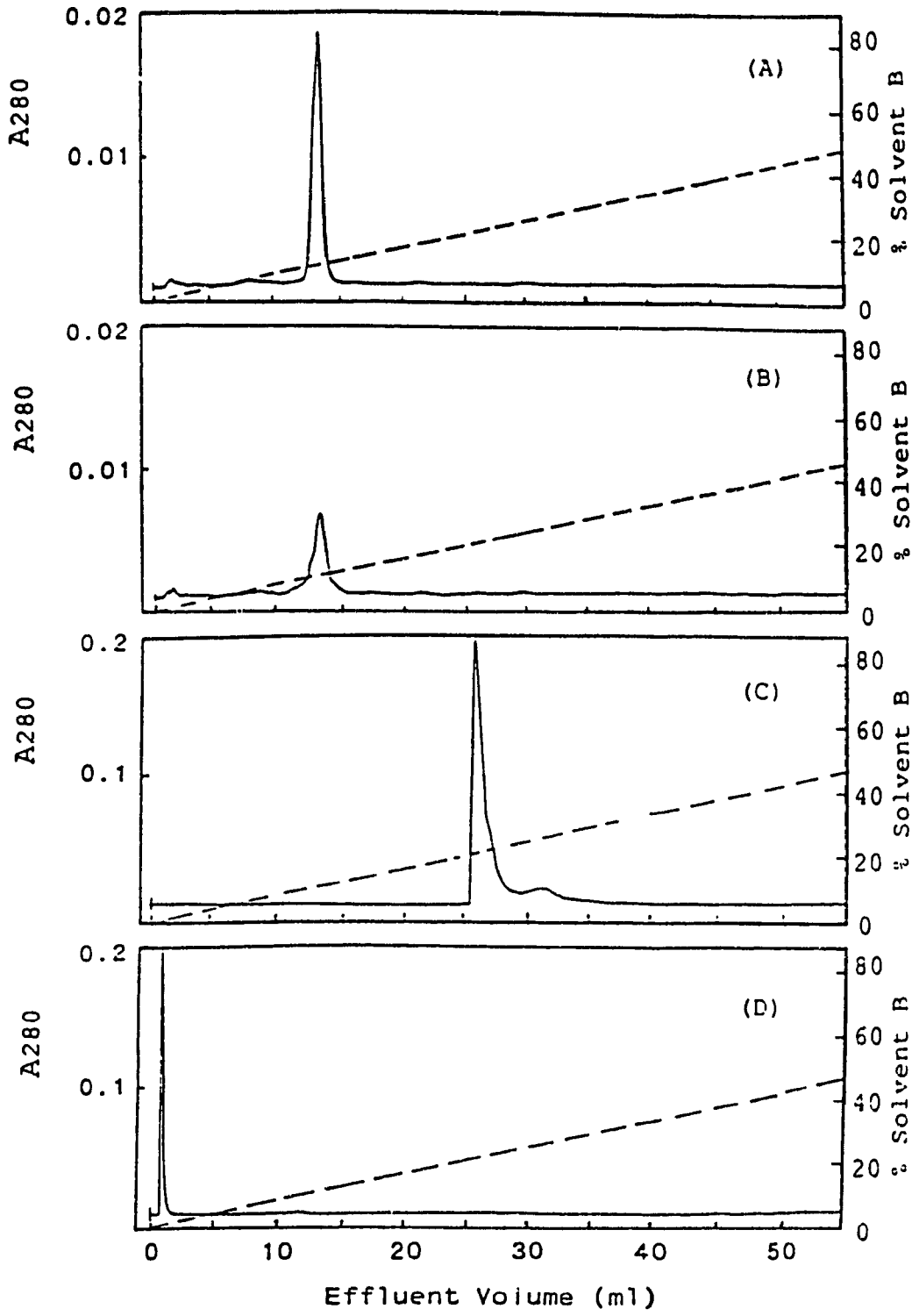

Fig.33. FPLC chromatograms of dcbpy and bpy. Column: PepRPC HR5/5. (A) dcbpy, pH 2.5; (B) dcbpy refluxed at 90 °C for 24 h, pH 2.5; (C) bpy, pH 8.0; (D) dcbpy refluxed at 90 °C for 24 h, pH 8.0. The FPLC conditions in (A) and (B) were the same as those in Fig.30 (A); those in (C) and (D) were the same as in Fig.31.

4. Discussion

The $Ru(dcbpy)_3^{4-}$ complex has several advantages for the study of biological electron-transfer reactions. The six carboxylate groups of $Ru(dcbpy)_3^{4-}$ are readily coupled to the amino groups of lysine residues of cyt c. Native horse heart cyt c has an isoelectric point of 9.4 [45] and a +7.5 charge at pH 7 [39]; the attachment of $Ru(dcbpy)_3^{4-}$ decreases the charge of cyt c so that $[(NN)_3Ru(Lys)]_2$cyt c, $(NN)_3Ru(Lys)$cyt c, and native cyt c can be separated by CM-Sepharose chromatography without difficulty. Only 1:1 and 2:1 Ru:heme derivatives were found, which is consistent with 2 major anion binding sites on cyt c [46]. The coupling reaction carried out at low ionic strength (10 mM Pi) so that coupling at electrostatically favourable sites was promoted. The mixture of $(NN)_3Ru(Lys)$cyt c derivatives was further purified by FPLC to yield singly-labelled derivatives. The major modification sites were found to be Lys 86 and 87, which are strongly implicated in the binding of cyt c to its biological partners [47] such as cyt c oxidase, peroxidase etc. [47]; thus, these Lys have high affinity for anion binding.

$Ru(dcbpy)_3^{4-}$ can be photoexcited to a metal-to-ligand charge-transfer (MLCT) excited state, Ru^{2+*}. $Ru(dcbpy)_3^{4-}$ and $(NN)_3Ru(Lys)$lysozyme show nearly identical emission intensity; thus the low emission intensity of the $(NN)_3Ru(Lys)$cyt c derivatives must be due to intramolecular quenching of the $^*Ru(dcbpy)_3^{4-}$ emission by the heme of cyt c.

Quenching can occur via energy transfer or electron transfer mechanisms:

$$^{*}Ru^{2+}\text{-}Fe^{3+} \xrightarrow{k_{en}} Ru^{2+}\text{-}Fe^{3+} \qquad (1)$$

$$^{*}Ru^{2+}\text{-}Fe^{3+} \xrightarrow{k_{el}} Ru^{3+}\text{-}Fe^{2+} \qquad (2)$$

Where k_{en} and k_{el} are the energy and electron transfer rate constants, respectively, and $k_q = k_{el} + k_{en}$.

Values for k_q, k_{el} and k_{en} have been reported for a number of $(bpy)_2(dcbpy)Ru(Lys)$cyt c derivatives [27, 28]. Table 15 shows these values, and the estimated distances between the ε-amino N of the modified Lys residues and the heme edge [27, 28]. There are two main differences between the values of k_q given in Tables 6 and 15. First, the maximum value of k_q for $(NN)_3Ru(Lys)$cyt c ($15 \times 10^6\ s^{-1}$) is less than that for the $(bpy)_2(dcbpy)Ru(Lys)$cyt c derivatives ($38 \times 10^6\ s^{-1}$). Second, the k_q values in Table 6 vary by only a factor of ~4 (3.8×10^6-$15\times10^6\ s^{-1}$), whereas the values for the $(bpy)_2(dcbpy)Ru(Lys)$cyt c derivatives vary by a factor of 76 (0.5×10^6-$38\times10^6\ s^{-1}$). The limited range of I/I_o, and hence k_q values, suggests that the modified lysines in the $(NN)_3Ru(Lys)$cyt c derivatives are clustered together.

The values of k_q for peaks 2-6 (Lys 86 modified) and 2-7 (Lys 87 modified) are 5.4×10^6 and 3.8×10^6, respectively. Assuming that the values of k_{en} for $(NN)_3Ru(Lys)$cyt c are the same as those for $(bpy)_2(dcbpy)Ru(Lys)$cyt c (i.e. $k_{en} = 2.5 \times 10^6\ s^{-1}$ for the Lys 86 derivative, and $1.7 \times 10^6\ s^{-1}$ for the Lys 87 derivative),

then k_{el} = 2.9 x 10^6 and 2.1 x 10^6 s^{-1} for $(NN)_3Ru(Lys)$cyt c modified at lys 86 and Lys 87, respectively. These values are significantly larger than those estimated for the corresponding $(bpy)_2(dcbpy)Ru(Lys)$cyt c derivatives (<10^5 s^{-1}) [28].

The theoretical expression for the electron-transfer rate constant was introduced by Marcus [48]:

$$k_{el} = 10^{13}\exp[-(\lambda+\Delta G^\circ)^2/4\lambda RT]\exp[-\beta(d-3)] \quad (s^{-1})$$

Where λ is the reorganization energy, ΔG° the reaction free energy, and d the distance from the donor to acceptor. The value of β varies between 0.9-1.2 $Å^{-1}$ [7, 8, 29]. The ΔG° for electron transfer in $(bpy)_2(dcbpy)Ru(Lys)$cyt c was estimated to be 0.98 based on $E^\circ(II^*/III)$ = -0.72 V for $Ru(bpy)_2(dcbpy)$ and E° = 0.26 V for cyt c [28]. No value for $E^\circ(II^*/III)$ for $Ru(dcbpy)_3^{4-}$ has been reported, so a ΔG° value for $(NN)_3Ru(Lys)$cyt c was not estimated, but it is expected to be similar.

The distance between the edge of the modified Lys residues and heme have been estimated [28] and these are also given in Table 15. Both theoretical and experimental results [7, 28] show that k_{el} is inversely related to the distances between the Ru^{2+} group and the heme. It is possible that the separation between Lys 86 and Lys 87 and the heme may be different in $(NN)_3Ru(Lys)$cyt c and $(bpy)_2(dcbpy)Ru(Lys)$cyt c since Lys residues have considerable flexibility. Therefore, different conformations are likely since $Ru(dcbpy)_3^{4-}$ has a larger volume and charge than $Ru(bpy)_2(dcbpy)$.

The values of k_q in Table 6 were calculated assuming $I/I_o = \tau/\tau_o$; thus, these

k_q's are only approximate values. More accurate values of k_q can be obtained by directly measuring τ using a pulsed laser system for excitation. Nevertheless, it is highly likely that the derivatives with higher k_q, e.g., peaks 2-9 (15×10^6 s^{-1}), 2-8 and 2-3 (9.7×10^6 s^{-1}), 2-5 (9.1×10^6 s^{-1}) are modified at Lys residues closer to the heme, i.e., Lys 13, 27, 72, 25 or 7.

Table 15: Values of k_q, k_{el}, k_{en}, and distance between the edge of the modified Lys residues and heme for $(bpy)_2(dcbpy)Ru(Lys)cyt\ c$ [a]

Lys modified	k_q[b]	k_{el}[b]	k_{en}[b]	Distance (Å)
86	2.5	<0.1	2.5	9-20
87	1.7	<0.1	1.7	10-22
13	22	16	6	6-10
72	18	14	4	6-12
8	3.2	<0.1	3.2	14-19
25	5.2	1.0	4.2	9-16
27	38	20	18	6-12
7	0.5	0.3	0.2	9-16
39	2.5	<0.1	2.5	12-15

[a] From Refs.27 and 28.

[b] Rate constants are given in units of 10^6 s^{-1}.

Appendices: FPLC Programs

Appendix 1. FPLC program used in Fig.17

```
0.00    CONC  %B     1.0
0.00    ML/MIN      0.50
0.00    CM/ML       0.40
0.00    MONITOR        1
0.00    ML/MARK      2.0
0.50    VALVE.POS    1.2
0.50    PORT.SET     6.1
0.50    CONC  %B     1.0
2.00    VALVE.POS    1.1
40.00   CONC  %B    12.0
55.00   CONC  %B    50.0
60.00   CONC  %B    50.0
```

Appendix 2. FPLC program used in Fig.19

```
0.00    CONC  %B     0.0
0.00    ML/MIN      0.50
0.00    LOOP TMS       3
0.00    CM/ML       0.40
0.00    VALVE.POS    1.2
0.00    CLEAR DATA
0.00    MONITOR        1
0.00    LEVEL  %     5.0
0.00    ML/MARK      2.0
0.00    INTEGRATE      1
0.25    PORT.SET     6.1
1.00    VALVE.POS    1.1
1.00    CONC  %B     0.0
1.00    CONC  %B     9.0
12.50   CONC  %B     9.0
12.50   CONC  %B     100
15.00   CONC  %B     100
15.00   INTEGRATE      0
15.00   CM/ML        0.0
15.25   PORT.SET     6.0
15.25   CONC  %B     100
17.50   CONC  %B     100
17.50   CONC  %B     0.0
20.00   CONC  %B     0.0
20.00   FEED TUBE
20.00   END OF LOOP
```

Appendix 3. FPLC program used in Fig.20

0.00	CONC %B	1.0
0.00	ML/MIN	0.50
0.00	CM/ML	0.40
0.00	MONITOR	1
0.00	ML/MARK	2.0
0.25	VALVE.POS	1.2
0.25	PORT.SET	6.1
0.25	CONC %B	1.0
2.00	VALVE.POS	1.1
22.00	CONC %B	18.0
22.00	CONC %B	100
25.00	CONC %B	100

Appendix 4. FPLC program used in Fig.24

0.00	CONC %B	0.0
0.00	ML/MIN	0.00
0.00	MONITOR	1
0.00	CM/ML	0.40
0.00	ML/MARK	2.0
0.25	VALVE.POS	1.2
0.25	PORT.SET	6.1
0.25	CONC %B	0.0
2.00	VALVE.POS	1.1
90.00	CONC %B	78.8

Appendix 5. FPLC program used in Fig.25

0.00	CONC %B	0.0
0.00	ML/MIN	0.00
0.00	MONITOR	1
0.00	CM/ML	0.40
0.00	ML/MARK	2.0
0.25	VALVE.POS	1.2
0.25	PORT.SET	6.1
0.25	CONC %B	0.0
2.00	VALVE.POS	1.1
90.00	CONC %B	70.0

Appendix 6. FPLC program used in Fig.26

0.00	CONC %B	0.0
0.00	ML/MIN	0.00
0.00	MONITOR	1
0.00	CM/ML	0.80
0.00	ML/MARK	0.20
0.25	VALVE.POS	1.2
0.25	PORT.SET	6.1
0.25	CONC %B	0.0
2.00	VALVE.POS	1.1
80.00	CONC %B	70.0

References

[1]. A.G. Mauk; R.A. Scott, and H.B. Gray, J.Am.Chem.Soc. 1980, 102, 4360.

[2]. D.G. Nocera; J.R. Winkler; K.M. Yocom; E. Bordignon, and H.B. Gray, J.Am.Chem.Soc. 1984, 106, 5145.

[3]. J.R. Winkler; D.G. Nocera; K.M. Yocom; E. Bordignon, and H.B. Gray, J.Am.Chem.Soc. 1982, 104, 5798.

[4]. S.S. Isied; G. Worosila, and S.J. Atherton, J.Am.Chem.Soc. 1982, 104, 7659.

[5]. S.S. Isied, C. Kuehn, and G. Worosila, J.Am.Chem.Soc. 1984, 106, 1722.

[6]. N.M. Kostic; R. Margalit; C. Che, and H.B. Gray, J.Am.Chem.Soc 1983, 105, 7765.

[7]. A.W. Axup; M. Albin; S.L. Mayo; R.J. Crutchley, and H.B. Gray, J.Am.Chem.Soc. 1988, 110, 435.

[8]. R. Bechtold, C. Kuehn, C. Lepre and S.S. Isied, Nature, 1986, 322(17), 286.

[9]. C. Che, R. Magralit, H. Chiang and H.B. Gray, Inorganica Chimica Acta, 1987, 135, 33.

[10]. J.L. Karas; C.M. Lieber, and H.B. Gray, J.Am.Chem.Soc. 1988, 110, 599.

[11]. M.P. Jackman; J. McGinnis; R. Powls; G.A. Salmon, and A.G. Sykes, J.Am.Chem.Soc. 1988, 110, 5880.

[12]. A.M. English, V.R. Lum, P.J. DeLaive, and H.B. Gray, J.Am.Chem.Soc., 1982, 104, 870.

[13]. B.S. Brunschwig, P.J. DeLaive, A.M. English, M. Goldberg, H.B. Gray, S.L.

Mayo, and N. Sutin, Inorg.Chem. 1985, 24, 3743.

[14]. J.L. McGourty, S.E. Peterson-Kennedy, W.Y. Ruo, and B.M. Hoffman, Biochem. 1987, 26, 8302.

[15]. H.D. Abruna, T.J. Meyer, and Y.W. Murray, Inorg. Chem. 1979, 18, 3233.

[16]. G. Sprintschnik, H.W. Sprinschnik, P.P. Kirsch, and D.G. Whitten, J.Am.Chem.Soc. 1977, 99, 4947.

[17]. O. Johansen, C. Kowala, A.W. Mau and W.H.F. Sasse, Australian J. Chem. 1979, 32, 1453.

[18]. J. Ferguson, A.W. Mau, and W.H.F. Sasse, Chem. Phys. Letts, 1979, 68, 21.

[19]. N. Sutin and C. Creutz, Advances in Chemistry Series, 1978, 168, 1.

[20]. W.R. Cherry and L.J. Henderson, Inorg.Chem. 1984, 23, 983.

[21]. P.J. Giordano, C.R. Bock, M.S. Wrighton, J.Am.Chem.Soc. 1977, 99, 3187.

[22]. H. Yamada, T. Imoto, K. Fujita, K. Okazaki, and M. Motomura, Biochem. 1981, 20, 4836.

[23]. J.W. Chase, B.M. Merrill and K.P. Williams, Proc.Natl.Acad.Sci. (U.S.A.) 1983, 80, 5480.

[24]. J.V. Staros, R.W. Wright, and D.M. Swingle, Anal.Biochem. 1986, 156, 220.

[25]. G.W. Bushnell, G.V. Louie, and G.D. Brayer, J.Mol.Biol. 1990, 214, 585.

[26]. P.D. Boyer ed., "The Enzymes", Vol.XI, 3rd edition, Academic Press, New York, 1975, p407.

[27]. L.P. Pan, B. Durham, J. Wolinska, and F. Millett, Biochem. 1988, 27, 7180.

[28]. B. Durham, L.P. Pan, J.E. Long, and F. Millett, Biochem. 1989, 28. 8659.

[29]. H. Elias, M.H. Chou, and J.R. Winkler, J.Am.Chem.Soc. 1988, 110, 429.

[30]. D.L. Brautigan, S. Ferguson-Miller, and E. Margoliash, Methods Enzymol. 1978, 53, 128.

[31]. G. Babul and E. Slellwagen, Biochem. 1972, 11, 1195.

[32]. T.K. Foreman, Ph.D. Dissertation, University of North Carolina, Chapel Hill, NC, 1982.

[33]. M.K. Nazeeruddin and K. Kalyanasundaram, Inorg. Chem. 1989, 28, 4251.

[34]. P. Yuan, H. Pande, B.R. Clark, and J.E. Shively, Anal. Biochem. 1982, 120, 289.

[35]. H.T. Smith, N. Staudenmayer, and F. Millett, Biochem. 1977, 16, 4971.

[36]. W. Fischli, A. Goldstein, M.W. Hunkapiller, and L.E. Hood, Proc. Natl. Acad. Sci. USA, 1982, 79, 5435.

[37]. M.T.W. Hearn and B. Grego, J. Chromatogr. 1983, 266, 75.

[38]. C.R. Cantor, P.R. Schimmel, and S.F. Freeman, "Biophysical Chemistry", Vol.2, Freeman, San Francisco, 1980, p77.

[39]. K.M. Yocom, Ph.D. Thesis, California Institute of Technology, 1982.

[40]. G. Allen, "Sequencing of Proteins and Peptides", 2nd edition, Elsevier, Amsterdam, 1989, p85.

[41]. S. Blackburn, "Enzyme Structure and Function", M.Dekker, New York, 1976, p106.

[42]. P.D. Boyer ed., "The Enzyme", Vol.III, 3rd edition, Academic Press, New York, 1971, p257.

[43]. G.E. Dunn and H.F. Thimm, Can.J.Chem. 1977, 55, 1342.

[44]. G.E. Dunn, E.A. Lawler, and A.B. Yamashita, Can.J.Chem. 1977, 55, 2478.

[45]. P.G. Righetti and T. Caravaggio, J.Chromatogr., 1976, 127, 1.

[46]. A.G. Sykes ed., "Advances in Inorganic and Bioinorganic Mechanisms", Vol.3, Academic Press, New York, 1982, 1-89.

[47]. G.W. Pettigrew and G.R. Moore, "Cytochromes c", Springer-Verlag, New York, 1987, p67.

[48]. R.A. Marcus and N. Sutin, Biochim. Biophys. Acta, 1985, 811, 265.